STRUCTURAL ANALYSIS PRACTICES FOR LARGE SCALE SYSTEMS

Robert H. Mallett* and Frederick W. Braun**
Bell Aerosystems, A Textron Company

Donald T. Hunter***
NASA Manned Spacecraft Center

Structural analysis practices that contribute to the effective analysis of large scale systems are described. The technical approach is via the matrix displacement method of structural analysis based upon finite element idealization. The context is a detailed thermal and mechanical stress analysis of the stacked Apollo Block II Spacecraft Lunar Module Adapter (SLA) and Service Module (SM). This structure is modeled in terms of 34 substructures which lead to an approximate total of 5000 finite elements and 15,000 displacement degrees-of-freedom. This refinement accounts for the complex variations in overall geometry, sizing dimensions, materials, thermal loading, mechanical loading, and boundary conditions. Embodied in the physical model are truss, frame, shear panel, triangular thin shell, quadrilateral thin shell, and triangular prism finite elements. The division into substructures of moderate size is put forward as a key to effective technical management of the stress analysis process.

*Chief, Advanced Structural Analysis
**Senior Numerical Analyst
***Structures Engineer

Report Documentation Page

Form Approved
OMB No. 0704-0188

1. REPORT DATE	2. REPORT TYPE	3. DATES COVERED
OCT 1968		**00-00-1968 to 00-00-1968**

4. TITLE AND SUBTITLE	5a. CONTRACT NUMBER
Structural Analysis Practices for Large Scale Systems	5b. GRANT NUMBER
	5c. PROGRAM ELEMENT NUMBER
6. AUTHOR(S)	5d. PROJECT NUMBER
	5e. TASK NUMBER
	5f. WORK UNIT NUMBER
7. PERFORMING ORGANIZATION NAME(S) AND ADDRESS(ES) **Air Force Flight Dynamics Laboratory,Wright Patterson AFB,OH,45433**	8. PERFORMING ORGANIZATION REPORT NUMBER
9. SPONSORING/MONITORING AGENCY NAME(S) AND ADDRESS(ES)	10. SPONSOR/MONITOR'S ACRONYM(S)
	11. SPONSOR/MONITOR'S REPORT NUMBER(S)

12. DISTRIBUTION/AVAILABILITY STATEMENT
Approved for public release; distribution unlimited

13. SUPPLEMENTARY NOTES
See also AD0703685, Proceedings of the Conference on Matrix Methods in Structural Mechanics (2nd) Held at Wright-Patterson Air Force Base, Ohio, on 15-17 October 1968.

14. ABSTRACT

15. SUBJECT TERMS

16. SECURITY CLASSIFICATION OF:			17. LIMITATION OF ABSTRACT	18. NUMBER OF PAGES	19a. NAME OF RESPONSIBLE PERSON
a. REPORT	b. ABSTRACT	c. THIS PAGE			
unclassified	**unclassified**	**unclassified**		**50**	

SECTION I

INTRODUCTION

Analysis support to the detailed design phase of the structural design process is usually provided at two levels. The first level of analysis is directed toward prediction of the internal load distribution. Then, these internal loads are employed in a second level analysis to obtain detailed stresses and associated margins of safety. The point of separation between these primary and secondary analyses depends upon the level of detail that can be achieved with the available primary analysis tools and within this constraint, the decision of technical management on the basis of a problem-oriented review of requirements and objectives.

Beam theory has been the mainstay of the primary analysis of many major missile and airframe components. As a consequence, the secondary detailed stress and margin of safety analyses have dominated the overall analysis effort. Powerful automated analysis systems, derived by implementation of the finite element technology, now provide the opportunity to shift the balance of the overall analysis effort to a refined primary analysis wherein some detailed stress data is obtained as well as an improved analysis of internal loads.

Pressure vessels for positive expulsion tankage represent one area in which a shift has taken place, to the extent that finite element analyses now dominate the analysis effort. Thin shell ring elements permit rapid and accurate prediction of the shell behavior. Three-dimensional stress state ring elements serve to supplement the thin shell analyses in regions of joints and attachments.

The realization of the potential of the finite element technology in the context of large scale built-up structures is a greater challenge. The use of finite element methods do not make analysis of such complex structures easier. Apart from the considerable investment of effort required to obtain a suitably general automated system, the definition, management, and interpretation of data are formidable problems.

A technical management decision to shift the balance of analysis effort from the largely manual secondary analysis to the primary analysis is governed by performance, schedule, and cost considerations. The advantage of the extended finite element primary analysis as regards to performance (accuracy) is generally accepted. The decisive factors then become schedule and cost, which are highly sensitive to proficiency in dealing with the data management problems mentioned above.

Powerful finite element structural analysis procedures have evolved at Bell Aerosystems. These have permitted a far-reaching integration of finite element analysis into company stress analysis practices. The balance of analysis effort has shifted toward the highly automated primary analysis phase. This improved analytical support of the design process has led to increased confidence in the resulting structural designs. It is the purpose of this paper to outline some of these practices by describing an application to Apollo Block II Spacecraft.

SECTION II

SPACECRAFT STRUCTURES

The Apollo Spacecraft is, as shown in Figure 1, functionally and structurally separable into Command (CM), Service (SM), Lunar (LM) and Adapter (SLA) Modules. Each of these modules taken individually, is a major structural system. It is clear from Figures 2 and 3 that each poses a substantial stress analysis problem when considered independently of the adjacent modules. Yet, the analysis described herein extends beyond this level of complexity to treat the stacked Service Module and Spacecraft Lunar Module Adapter (SM/SLA) as a single unit. Internal loads, detailed stresses, and margins of safety are sought under thermal and inertial loading at the end of first stage boost (End-Boost).

At the outset of this analysis, extensive consideration was given to establishing a feasible optimum balance of effort between the automated finite element primary analysis and the largely manual secondary analysis. The factors considered included the basis and results of existing stress analyses, the difficulty of manually working internal loads down to detailed stresses in the presence of thermal loading, and the emphasized high accuracy objectives.

The result of the foregoing deliberations was a decision to use the full resources of the available automated finite element analysis system in an attempt to obtain detailed stresses and associated margins of safety within the scope of the primary analysis. Only attachments, joints, and cutouts were expressly deferred to the secondary analysis phase.

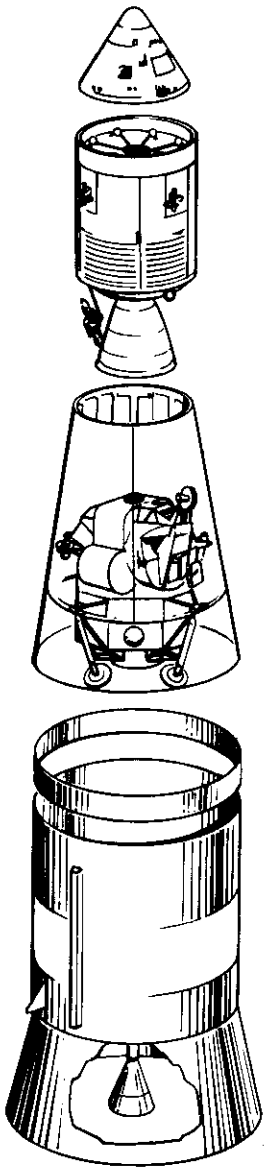

Figure 1. Apollo Short Stack

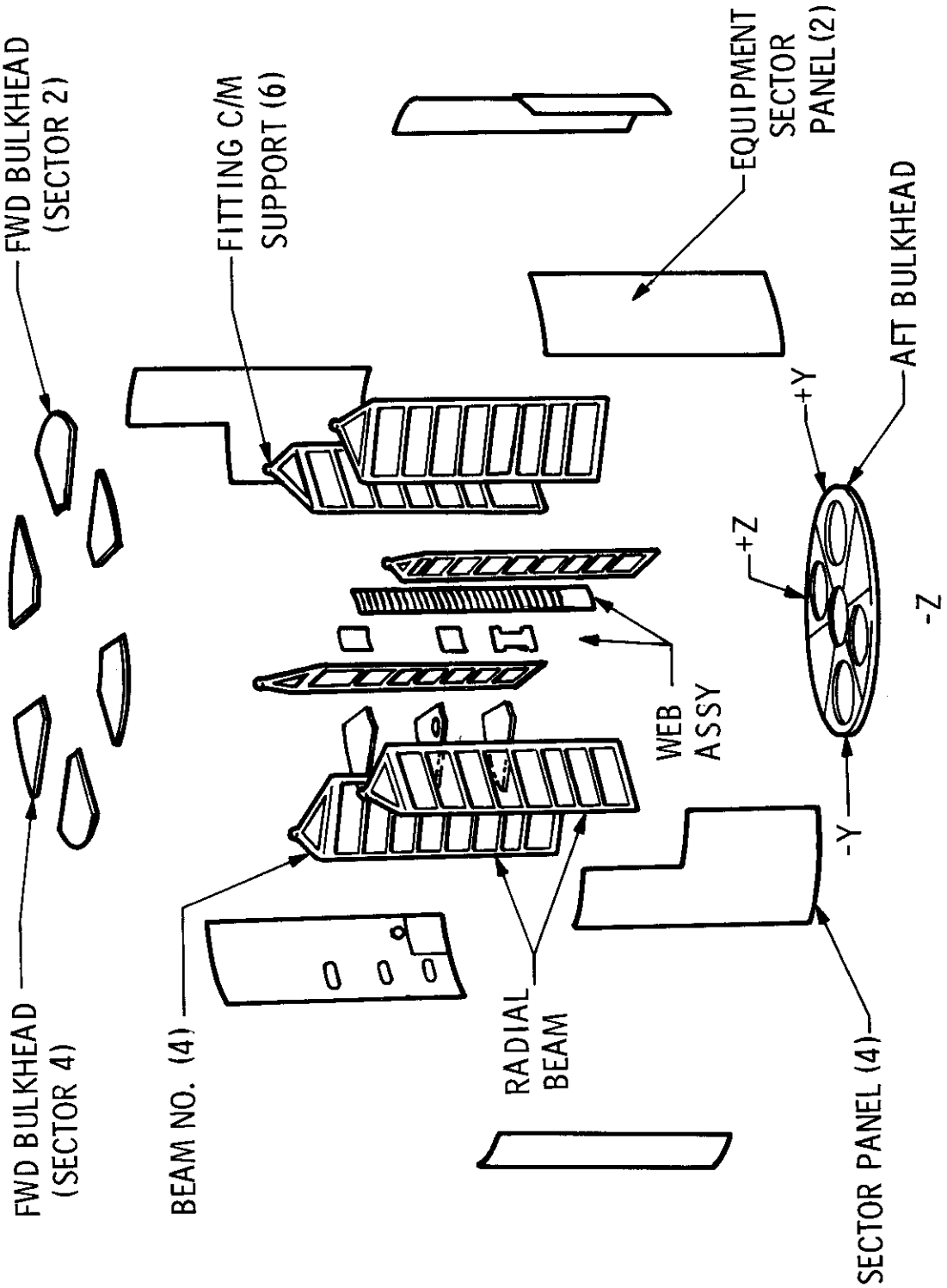

Figure 2. Structural Assembly

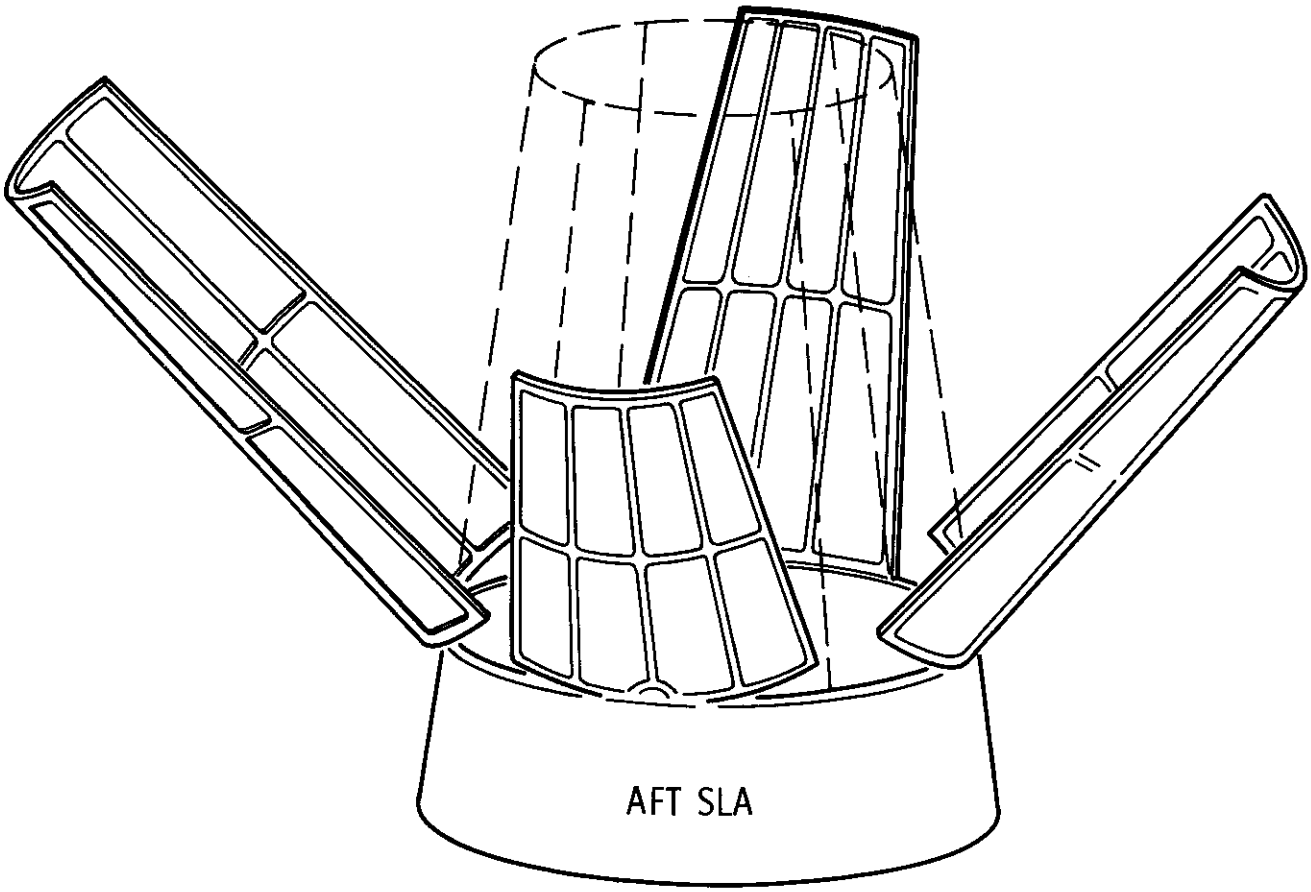

Figure 3. SLA Structural Assembly

The successful execution of this plan is presented in detail in References 1 and 2, and outlined herein. Section II discloses that the analysis procedure employed to deal with the SM/SLA Structure is based upon substructuring. The basic matrix algebra of this procedure is well known; however, its systematic utilization in actual practice is thought to represent an advance in the state of the art. Accordingly, emphasis herein is placed upon the impact of substructuring upon structural analysis practices.

Section III is devoted to description of the Bell automated system for structural analysis. The availability of this system was prerequisite to the course of action taken in the analysis of the SM/SLA Structure. Project schedules seldom permit but little capability development.

The finite element model is described in Section IV in terms of the idealized structure, applied loading and boundary conditions. The highly refined model that was defined to meet

the primary analysis objectives has the following approximate size characteristics: 34 substructures, 5000 finite elements, 3000 gridpoints, and 15,000 displacement degrees of freedom.

Sufficient results are presented in Section V to demonstrate the validity of the analysis performed. Expectations were exceeded. Gross force balance checks exhibit negligible error. Predicted stress distributions readily permit rational interpretation. Conclusions are recorded in Section VI. Collectively, these assert the successful performance of the analysis of the SM/SLA Structure and therewith the evolution of satisfactory structural analysis practices for large scale systems.

SECTION III

THE ANALYSIS PROCESS

GENERAL

A primary attraction of the matrix methods of structural analysis is that many significant problems can be solved with very modest computer programs. In the simplest case, a capability to generate and assemble a certain type of element stiffness matrix and solve the resulting system stiffness equation is sufficient. On the other hand, the automated analysis systems required to cope with the SM/SLA class of structure in a practical design situation bear little relation to the type of finite element computer program mentioned above. Practical analysis tools must be implemented as an integral part of the overall structural analysis and design cycle.

Powerful automated analysis tools have been derived from finite element technology. These tools enable the conduct of broad classes of analytical analysis and design studies which focus almost exclusively upon the relevant phenomenological aspects. For these problem classes, sophisticated behavior predictions are available without recourse to tedious and time consuming manual algebraic and numerical computation or special computer program development.

The thermal stress analysis of the SM/SLA Structure reported herein is an example of a study for which an applicable basic analysis system was available. The following paragraphs present the conceptual basis for this analysis system.

The automated analysis system employed to carry out the thermal stress analysis of the SM/SLA Structure was guided in its evolution by a consideration of structural analysis practices. These practices, the automated analysis system and the inherent matrix algebra are discussed together as the analysis process applied to the SM/SLA Structure.

It is apparent from the size and complexity of the SM/SLA Structure that a great deal of data is involved. The detailed design specification of the structure is spread over numerous drawings and through many documents. A realistic physical model necessitates thousands of gridpoints and finite elements. Translated into computer program input, related data items include coordinates of all gridpoints, degree of freedom specifications for all gridpoints, connection specifications for all finite elements, and others. This volume of input data implies a need for many hours of computer time for numerical solution. Finally, extensive output inevitably results from such an analysis.

Effective management of the voluminous data associated with large scale structure was the decisive consideration in establishing the basic analysis process. For this reason, the analysis is performed by substructuring and proceeds in four major phases.

Phase I is concerned with the individual substructures of the total SM/SLA Structure. In the Phase I analysis, each substructure is considered individually. Input data is prepared and calculation is carried forward to determine matrix representations referenced to the interfaces.

Phase II considers the structure as a whole. The interface stiffness matrices for the individual substructures are assembled and the complete set of interface displacements is determined.

Based upon interface displacements obtained from Phase II and auxiliary information from the individual Phase I analysis, Phase III completes the conventional finite element analysis. Each substructure is considered in turn. Prediction of the primary displacement variables is completed and secondary variables such as forces and stresses are calculated.

Phase IV is a nonintegral step designed to translate the conventional Phase III results into a form desired by the stress analyst and carries out the determination of margins of safety. Phase IV completes the finite element analysis process employed for the thermal stress analysis of the SM/SLA Structure. Each of these phases is described in detail in the following subsections.

PHASE I

The matrix algebra of the Phase I analysis is deceptively straightforward when reduced to the essential calculations relevant to the primary displacement variables and stripped of the problematical data storage and retrieval steps inherent in the computer program. However, the simplified symbolic statement of the process is considered appropriate in the present context. Accepting this viewpoint, the first step of the Phase I analysis process yields potential energy expressions for the individual finite elements given by

$$\Phi_{pe} = \frac{1}{2} \left\lfloor \delta_e \right\rfloor \left[K_e \right] \left\{ \delta_e \right\} - \left\lfloor \delta_e \right\rfloor \left\{ F_e \right\} \tag{1}$$

where

$\left[K_e \right]$ is the element stiffness matrix,

$\left\{ \delta_e \right\}$ is the relevant gridpoint displacement vector, and

$\left\{ F_e \right\}$ is the element total applied load vector.

These individual element potential energies are then assembled to form a potential energy expression for the substructure under consideration.

$$\Phi_p = \frac{1}{2} \left\lfloor \delta \right\rfloor \left[K \right] \left\{ \delta \right\} - \left\lfloor \delta \right\rfloor \left\{ F \right\} \tag{2}$$

where

$\left[K \right]$ is the substructure stiffness matrix

$\left\{ \delta \right\}$ is the substructure displacement vector, and

$\left\{ F \right\}$ is the total substructure applied load.

The Phase I analysis is carried forward by rewriting the substructure potential energy in partitioned form to reflect the division between interior gridpoint degrees of freedom $\{\delta_i\}$ and interface (boundary) gridpoint degrees of freedom $\{\delta_b\}$ i.e.

$$\Phi_p = \frac{1}{2}\left[\delta_i \;,\; \delta_b\right]\begin{bmatrix} K_{ii} & , & K_{ib} \\ K_{ib}^T & , & K_{bb} \end{bmatrix}\begin{Bmatrix}\delta_i \\ \delta_b\end{Bmatrix} - \left[\delta_i \;,\; \delta_b\right]\begin{Bmatrix}F_i \\ F_b\end{Bmatrix} \tag{3}$$

Contributions to the potential energy which stem from the interior gridpoints are complete while additional contributions will be added in at the interface gridpoints upon assembly of the substructures. Advantage is taken of the completeness at the interior points by solving for these displacement degrees of freedom in terms of the interface degrees of freedom. The result is given by,

$$\{\delta_i\} = [K_{ii}]^{-1}\{F_i\} - [K_{ii}]^{-1}[K_{ib}]\{\delta_b\} \tag{4}$$

Substitution of this relation into Equation 3 yields the objective substructure potential energy expression referenced to interface degrees of freedom,

$$\Phi_{pb} = \frac{1}{2}\left[\delta_b\right]\left[K_b\right]\{\delta_b\} - \left[\delta_b\right]\{P_b\} \tag{5}$$

where

$$\left[K_b\right] = \left[K_{bb} - K_{ib}^T \quad K_{ii}^{-1} \quad K_{ib}\right] \tag{6}$$

$$\{P_b\} = \{F_b\} - \{K_{ib}^T \quad K_{ii}^{-1} \quad F_i\} \tag{7}$$

$[K_b]$ is the substructure interface stiffness matrix,

$\{\delta_b\}$ is the substructure interface displacement vector, and

$\{P_b\}$ is the substructure interface load vector.

The individual substructure potential energy expressions of the form defined in Equation 5 are the basic Phase I analysis results required to construct the governing stiffness equation for the entire structure in the Phase II analysis process.

The foregoing statement of the Phase I analysis process actually implies a complete general purpose computer program for stress analysis plus the capability to form and store such items as interface stiffness matrices on magnetic tape for subsequent access. It is instructive to take the viewpoint of the structural analyst and reexamine the Phase I analysis process as an application of the automated general purpose analysis system.

By definition, Phase I proceeds against a number of substructures of the SM/SLA Structure although inclusion of the complete structure within a single substructure would yield a conventional one-pass linear stress analysis. The reasons for division of a structure such as the SM/SLA into multiple substructures are many and varied. Unnecessary breakdown into substructures is, of course, inefficient.

A primary reason for substructuring stems from the fact that it is efficient to confirm a large quantity of input data via subsets. With substructuring, an analyst can focus his attention upon a limited region or component in specifying input data. This subset of data can then be processed through data checking executions. Such executions involve only the relatively small quantities of data of current interest with the result that turn-around is rapid and inexpensive.

Substructuring can also shorten the calendar time required to confirm the input data for a large structure. The reason is that substructuring facilitates distribution of the input data specification effort to a number of analysts for nearly independent simultaneous preparation. It is worth mentioning that the automatic generation of structural plots from the input data is an important aid to the confirmation of input. Plots of the structural components taken individually are desirable.

The benefits of substructuring large scale structures extend beyond the input data confirmation stage through execution. The effective matrix banding may be improved by substructuring. Long continuous executions are avoided. Numerous restart points are automatically provided. Most important, the Phase I executions are spread over the period of time required to complete the specification of data for all the component substructures. Executions in the succeeding phases may be similarly spread to generate results paced by progress in evaluation.

Substructuring is particularly advantageous when localized modifications in structure or applied loading arise subsequent to the analysis. Such modifications can often be accommodated by re-analysis of only those substructures affected.

Having discussed the motivation for and the scope of the Phase I analysis, the following paragraphs focus upon the several steps involved. Preprinted input forms are employed to simplify the specification of input data. These forms are designed to provide automatic internal generation of data whenever possible. For example, repetitious data need only to be specified initially followed by any exceptions.

The built-in data generation features were supplemented in analysis of the SM/SLA Structure by auxilliary data generation programs. For example, a simple but useful auxilliary program was written to generate the gridpoint coordinates with reference to a global rectangular set of coordinate axes. Of course, inplane and normal coordinate directions were ultimately employed for the degrees of freedom on the shell surfaces.

The first executions of the automated analysis system are undertaken to confirm the input data deck as discussed earlier. The deck is read and the implied data is generated explicitly. Consistency of the data is checked and all data items are stored for execution restart and printed for further checking by the analyst. In addition, a magnetic tape is generated for automatic plotting of the finite element model.

Upon acceptance of the input data specification by the analyst, the actual Phase I analysis is undertaken for the substructure under consideration. This analysis is a complete linear stress analysis of the substructure under the assumption that the interface displacements are completely fixed. The output obtained from this analysis provides further important confirmation of the finite element model. Moreover, these results often provide useful preliminary information about the behavior of the substructure.

In addition to the preliminary stress analysis results, the Phase I analysis generates and stores the interface referenced stiffness and applied load matrices as well as the other information required in subsequent analysis phases.

PHASE II

The Phase II analysis begins with the substructure interface matrices from Phase I and carries the analysis process through prediction of the interface displacement variables. Phase II is the only part of the analysis process which deals with more than one substructure at a time.

The substructure potential energy expressions (Equation 5) are the point of departure. Such an expression is known for each substructure, for example

$$\Phi_{pb}^{(j)} = \frac{1}{2}\left[\delta_b^{(j)}\right]\left[K_b^{(j)}\right]\left\{\delta_b^{(j)}\right\} - \left[\delta_b^{(j)}\right]\left\{P_b^{(j)}\right\} \qquad j = 1, 2, \cdots n. \tag{8}$$

The interface displacements pertinent to each substructure $\{\delta_b^{(j)}\}$ are known as elements of the total list of interface displacements $\{\Delta\}$ for the assembled structure. This relationship is expressible mathematically by a Boolean transformation.

Symbolically,

$$\{\delta_b^{(j)}\} = [\Gamma_a^{(j)}]\{\Delta\} \tag{9}$$

Introduction of this transformation into the set of independent interface displacement degrees of freedom for the total structure yields

$$\Phi_{pb}^{(j)} = \frac{1}{2}\lfloor\Delta\rfloor [K^{(j)}]\{\Delta\} - \lfloor\Delta\rfloor \{P^{(j)}\} \qquad j = 1, 2, \cdots n. \tag{10}$$

where

$$[K^{(j)}] = [\Gamma_a^{(j)}]^T [K_b^{(j)}][\Gamma_a^{(j)}] \tag{11}$$

$$\{P^{(j)}\} = [\Gamma_a^{(j)}]^T \{P_b^{(j)}\} \tag{12}$$

The substructure interface potential energy expressions of the form of Equation 10 are added to obtain the complete potential energy for the structure

$$\Phi_p = \frac{1}{2}\lfloor\Delta\rfloor [K]\{\Delta\} - \lfloor\Delta\rfloor \{P\} \tag{13}$$

where

$$[K] = \sum_j [K^{(j)}] \tag{14}$$

$$\{P\} = \sum_j \{P^{(j)}\} \tag{15}$$

The formality of transforming to conformable substructure matrices before assembly of the total structure matrices is avoided in actual practice. Instead, a noncomformable sum is effected to obtain Equation 13 directly from Equation 8.

The objective equation governing displacement of the interface points follows immediately by executing the variation of the potential energy expression of Equation 13. The result, retaining the symbolism of a single load condition, is given by,

$$[K]\{\Delta\} = \{P\} \tag{16}$$

Frequently the number of substructures assembled into the Phase II analysis is greater than the number generated in the Phase I analysis. This increase stems from two sources.

Duplication of physical components is the source encountered most frequently. The Phase I generation of interface referenced matrices need only be executed once for identical substructures. This one set of results is then assembled as often as the substructure occurs. Proper placement is achieved through individual specification of the interconnection transformation in Equation 9. Large scale finite element models with extensive repetition of subassemblies can be effectively transformed into small problems using this approach.

The second source of additional substructures at Phase II is direct card input of known matrices. The origin of such matrices is not particularly important. Care must be taken to insure that the given matrices are expressed in conformable degrees of freedom. Additional substructures derived from both of these sources participated in the Phase II analysis of the SM/SLA Structure.

The total interface matrix $[K]$ is a symmetric matrix that is stored in banded form. Solution is effected by triangularization of the matrix and backsubstitution for the set of interface displacement variables appropriate to each load condition.

For most structures the division between the Phase I and Phase II analysis phases is little more than a convenient point for execution interruption to avoid long continuous machine runs. A relatively small amount of input data is required at this point. This was not the case for the SM/SLA Structure. In this instance, the substructure file tape generated during Phase I for input into Phase II could not contain all the Phase I results. Therefore, intermediate runs were required to build a Phase II input tape with all nonessential data deleted.

The values obtained in Phase II for the interface displacements are stored on magnetic tape for access during the Phase III analysis. In most cases, exit from Phase II need only be viewed as a convenient point for execution interruption. However, in the case of the SM/SLA Structure it was necessary to generate punched cards for the interface displacement solution and initiate Phase III from Phase I result tapes because information was deleted from the substructure file tape prior to Phase II. Thus, Phase II was forced to terminate with the punched card solution for the interface displacements.

PHASE III

From the structure file tape, Phase III picks up the matrix descriptions of the individual substructures generated in Phase I and the solution for the interface displacements from Phase II and carries the analysis process forward. Firstly, the relevant interface displacements are extracted from the complete set (Equation 9). Then, the interior displacements are calculated using Equation 4.

$$\{\delta_i\} = [K_{ii}]^{-1}\{F_i\} - [K_{ii}]^{-1}[K_{ib}]\{\delta_b\} \tag{17}$$

With this result all the primary variables for a given substructure are known and various secondary items are computed. For example, stresses are available for each finite element in the substructure via a relationship of the form

$$\{\sigma\} = [S]\{\delta\} - \{s\} \tag{18}$$

where

$\{\sigma\}$ is the element stress vector,

$[S]$ is the element stress matrix, and

$\{s\}$ is the thermal stress correction vector.

Many useful additional items are calculated in Phase III in the general purpose analysis system employed. Included are: element forces, reactions, force balance, and energy values. Even so, this information falls short of that desired for detailed stress and margin of safety determinations. This gap between conventional finite element stress analysis results and the information desired by the stress analyst occasioned the extension of the automated analysis process to include a Phase IV.

PHASE IV

Phase III computes the normal finite element results for substructures specified by the stress analyst. These results are stored on magnetic tape as well as printed. This magnetic tape furnishes the primary input data for the Phase IV analysis. Phase IV is initiated immediately following Phase III or after examination of the printed results from Phase III at the discretion of the stress analyst.

The computations of Phase IV are designed to reduce automatically the predicted behavior data for evaluation by the stress analyst in terms of margins of safety. A typical computation of this automatic reduction process is the consideration of tensile yielding. This involves the interpolation of the allowable stress from the appropriate temperature referenced table on a magnetic tape file. Then, the equivalent stress is calculated from the actual multiaxial stress state. This equivalent stress state is interpreted via Von Mises yield criterion for comparison with the allowable stress. Comparison is made quantitatively in terms of a margin of safety. The results of this comparison are printed with explicit labeling and an asterisk (*) is employed to identify all negative margins of safety.

The automatic data reduction of Phase IV extends beyond the check against Von Mises yielding to include consideration of various margins of safety against limit and ultimate load. The reader is referred to the primary Stress Report of Reference 2 for further description of the automatically generated stress report output sheets.

SECTION IV

THE AUTOMATED ANALYSIS SYSTEM

ORGANIZATIONAL CHARACTERISTICS

A conceptual organization of the Bell general purpose analysis system is shown in Figure 4. This system provides a powerful capability for static linear analysis of complex large scale structures as well as for various nonlinear and time dependent applications.

The organization chart of Figure 4 illustrates the division into distinct functional modules which is fundamental to general purpose program organization. The extension of the concept to the higher level "library" modules shown in Figure 4 builds in optional groups of basic modules. Five such libraries are included in the Bell general purpose analysis system employed for the SM/SLA Structure. These are described individually in the following subsections.

1. The Execution Library

The execution library builds in alternative analysis procedures. Figure 5 lists those included in the Bell general purpose system for structural analysis. This broad variety of analyses actually embody relatively few computations that are unique: rather, an extensive commonality exists that enables efficient development and operation of automated general purpose analysis systems.

2. The Problem Library

The problem library takes the form of a magnetic tape prepared for the analyst. This problem library serves as the substructure file tape in analyses that embody substructuring.

The primary benefits of a problem library are those cited earlier as accruing from substructuring. While essential to substructuring, the problem library also provides important advantages in the analysis of intermediate size (single substructure) problems. In particular, the problem library facilitates execution interruption, restart, and provides a compact functional record. Restart can be invoked to examine modified designs and alternative loadings. Generally, the problem library allows flexibility of operation to the analyst.

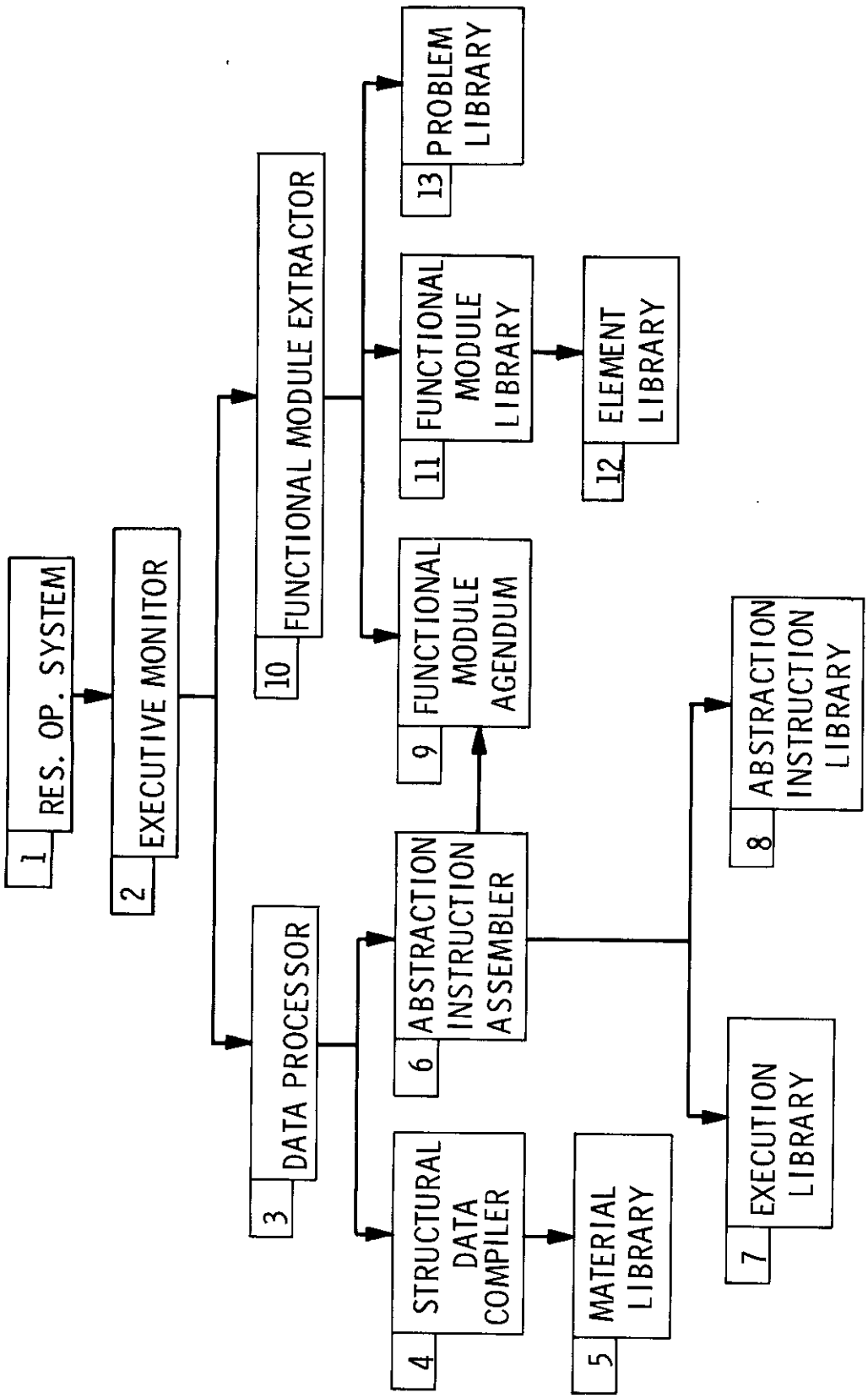

Figure 4. Computer Program Organization

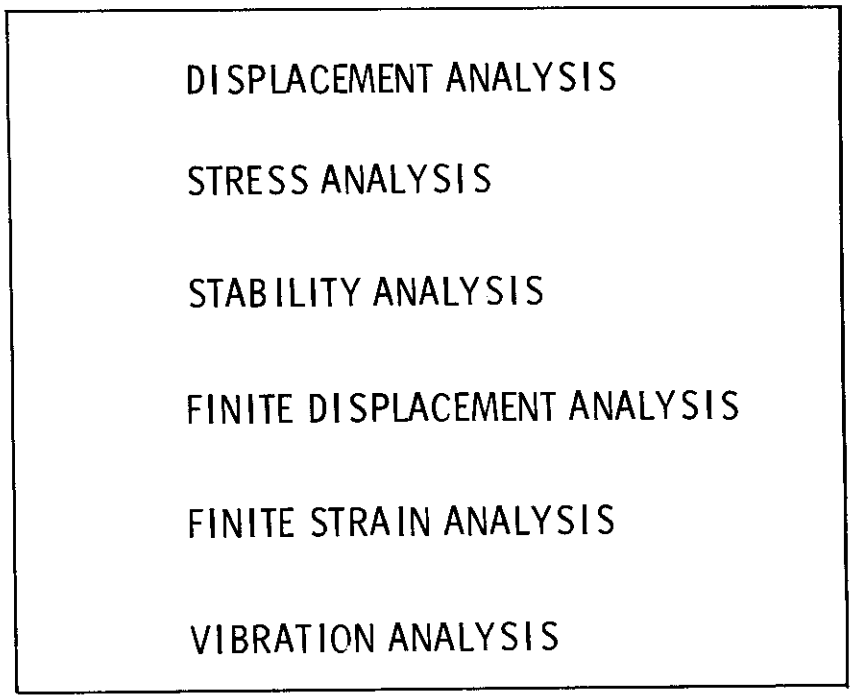

Figure 5. Analysis Procedures

3. The Material Library

The material library takes the form of a magnetic tape which is a permanent data set available for interrogation by the analysis system. A complete set of temperature referenced properties for a material constitutes an entry in the material library. The items which make up an entry are listed in Figure 6. Provision is made for up to nine temperature levels. Linear interpolation is employed to obtain values at any specified temperature level.

Control of the material tape as regards additions, modifications and deletions resides with the analyst. Access to the material tape for such updating may be taken independently of, or in connection with, application of the analysis system.

4. The Utility Library

The utility library is an elementary interpretive system in the form of a collection of Fortran IV Subroutines. Computational routines common to several element matrix generation procedures are placed in the utility library to avoid a duplication of programming.

ITEM	TEMPERATURE REFERENCED DATA
1	ORTHOTROPIC ELASTIC CONSTANTS
2	ORTHOTROPIC THERMAL COEFFICIENTS
3	ORTHOTROPIC YIELD VALUES
4	ORTHOTROPIC STRUCTURAL DAMPING COEFFICIENTS
5	STRAIN HARDENING PARAMETERS
6	MASS DENSITY

Figure 6. Material Library Entry List

5. The Finite Element Library

The finite element library is the heart of the automated analysis system. The set of finite element models available in this library is listed in Figure 7. A call on this library causes the appropriate element matrices to be generated. A complete set of matrices for a finite element model is listed in Figure 8.

The types of element models incorporated in the finite element library determines the applicability of the analysis system to different classes of structures. The matrices included in the element representations determine the type of analyses that can be performed. The finite element library incorporated in the Bell general purpose analysis system provides a capability to model most structures. The subject SM/SLA Structure is a good illustration of this versatility.

SIZE CHARACTERISTICS

The foregoing comments have described the general framework of the automated system employed in the analysis of the SM/SLA Structure. Subsequent comment in this subsection is devoted to description of its size characteristics and certain special operational features.

The size characteristics of the Bell general purpose analysis system are twofold. There are size characteristics of the program itself and of its problem solving capability. Considering the former, the analysis system contains 335 subroutines (approximately 30,000 source cards) logically designed into 51 overlay links on an IBM 7090 with 32K words of storage. This analysis system requires a minimum of 18 external storage units.

IDENT. NO.	DESIGNATION
10	TRUSS
11	FRAME
20	HELLE TRIANGULAR THIN SHELL
21	MALLETT QUADRILATERAL THIN SHELL
22	BELL TRIANGULAR THIN SHELL
23	BELL QUADRILATERAL THIN SHELL
24	QUADRILATERAL SHEAR PANEL
30	TOROIDAL THIN SHELL RING
40	TRIANGULAR CROSS SECTION RING
41	TRAPEZOIDAL CROSS SECTION RING
42	CORE
50	TETRAHEDRON
51	TRIANGULAR PRISM
52	RECTANGULAR PRISM

Figure 7. Finite Element Library

The scale of the problem solving capability is virtually unlimited from the viewpoint of storage requirements although the maximum size of an individual substructure is restricted to "on the order of" 2000 displacement degrees of freedom. Other relevant maximum storage size constraints for an individual substructure are 1000 finite elements, 1000 gridpoints, 35 materials and 9 load conditions.

MATRIX	IDENTIFICATION
M	CONSISTENT MASS
D_v	VISCOUS DAMPING
D_s	STRUCTURAL DAMPING
K	STIFFNESS
N	INCREMENTAL STIFFNESS
F_{pf}	FIELD PRESSURE LOAD
F_{pc}	BOUNDARY PRESSURE LOAD
F_ϵ	PRESTRAIN LOAD
F_T	THERMAL LOAD
F_σ	PRESTRESS LOAD
S	STRESS
Δ	STRESS CORRECTION

Figure 8. Finite Element Matrices

SECTION V

THE SM/SLA IDEALIZATION

THE FINITE ELEMENT MODELS

Six types of finite elements participate in the idealization of the SM/SLA Structure. These are illustrated in Figure 9. In-depth descriptions of these finite elements are given in Reference 1.

The frame element, shown in Figure 9a, finds application in the SM/SLA Structure in modeling stiffening components. The stiffening of the SM/SLA Structure is generally eccentric to the midsurface of the shell. The frame element matrices account for the eccentricities.

The shear panel finite element, shown in Figure 9b, is employed in idealization of the webs in the radial beams of the SM Structure, since these webs carry load primarily by diagonal tension. The direct load carrying capacity of the webs is delegated to surrounding frame members.

The quadrilateral thin shell element, shown in Figure 9c, is a basic building block in the finite element model of the SM/SLA Structure. This element is specialized to a membrane element to model such components as the closeouts of the SM aft bulkhead in addition to its general usage in modeling the primary sandwich shells of the SM/SLA Structure.

The triangular thin shell element, shown in Figure 9d, is used extensively in the finite element model of the SM/SLA Structure. This element is a compatible companion to the quadrilateral thin shell element and is often employed only in small numbers in regions of irregularity. However, in the SM/SLA Structure the high degree of irregularity in both structure and loading is reflected in a highly variable finite element gridwork embodying an unusual proportion of triangular elements.

The configuration of the SM/SLA Structure is described by the outer sandwich shells of revolution. Ideally, the foregoing finite element building blocks would also embody curvature. However, a suitably curved element is beyond the present state of the art and thin shell elements of zero curvature work effectively. An element of zero curvature remains a bonafide thin shell element in the sense that both membrane and flexure actions are incorporated in the element representations.

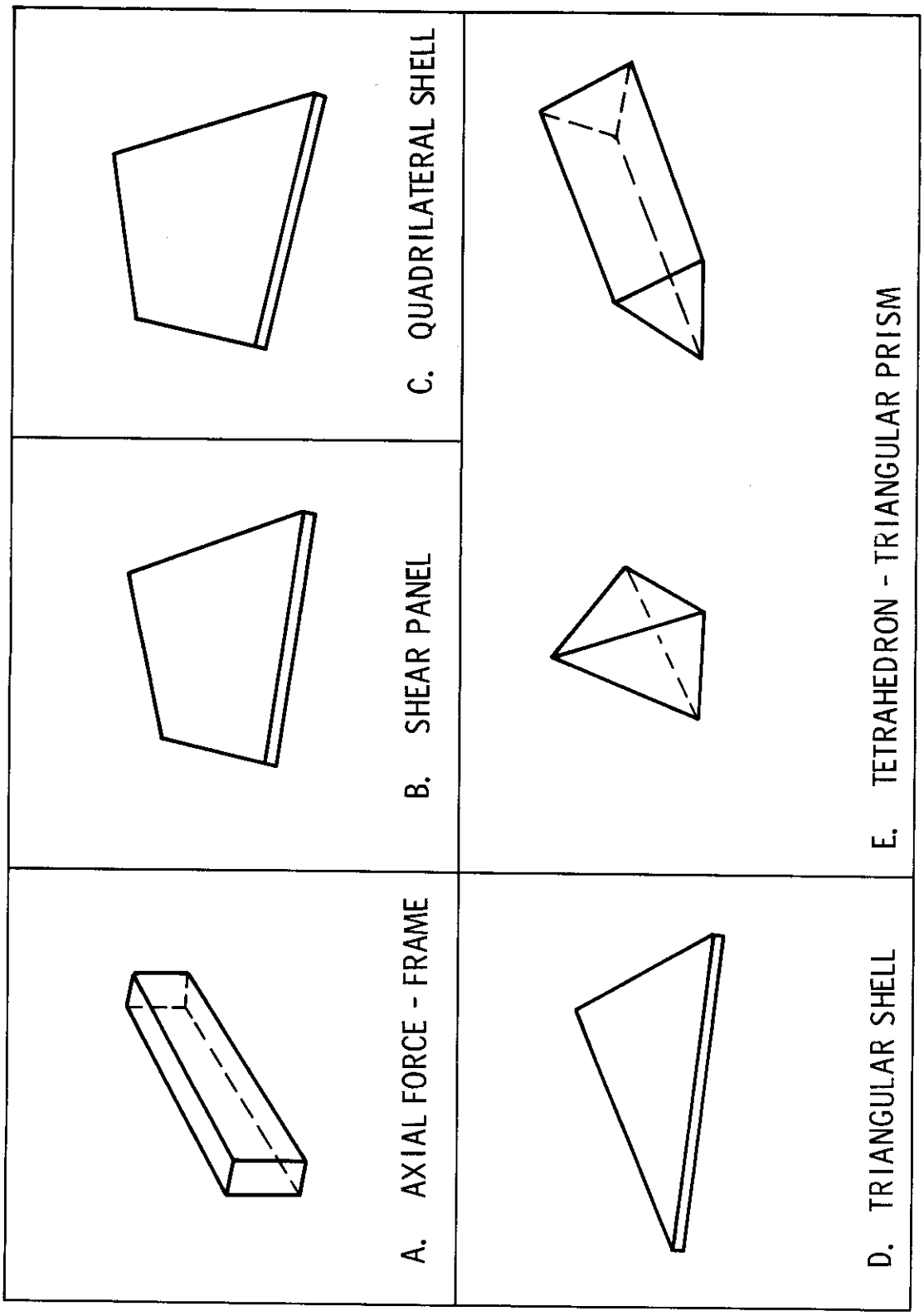

Figure 9. Finite Elements

The triangular prism element, shown in Figure 9e, is employed to model the variable anisotropic shear core in the aft bulkhead of the SM Structure. This versatile element is useful for the idealization of solid structure. It is formed from a built-up assembly of three or more basic solid elements of tetrahedron shape. The tetrahedron is also available as a separate element for filling in regions of irregularity but was not required for the SM/SLA Structure.

THE SM/SLA MODEL

Idealization of the SM/SLA Structure proceeds in two steps consistent with the analysis process of Section II. Firstly, the breakdown into substructures is defined. Then, each substructure, considered individually, is idealized in terms of finite elements.

The basic breakdown into substructures is effected along interface lines between major structural components. These components are further subdivided to obtain units of manageable size. In this process an attempt is made to isolate within a single substructure any regions anticipated to require subsequent reanalysis.

Reference to the SLA Structure of Figure 10 clarifies the procedure followed in definition of substructures. The single lines are the interface lines between the major physical components of the SLA Structure. The dashed lines disclose the breakdown into substructures. Note that this subdivision is defined to facilitate reanalysis of the built-up area beneath the LM attachment points and the area of the interface with the SM Structure. Note also that this breakdown into substructures is defined so as to obtain repeatable substructures.

The division of the individual substructures into finite elements determines the attainable level of accuracy of the analysis. The minimum acceptable refinement is regarded as that required to yield satisfactory stiffness characteristics at the substructure boundaries. This permits subsequent refined analyses to focus exclusively on the substructure in question.

The maximum level of refinement of a substructure is regarded as that which possesses sufficient gridpoints to permit interpolation of the applied load distributions and the anticipated stress distributions. Refinement at this level was attempted throughout the SM/SLA Structure to obtain meaningful detailed stresses and associated margins of safety. No subsequent refined reanalyses were planned nor required.

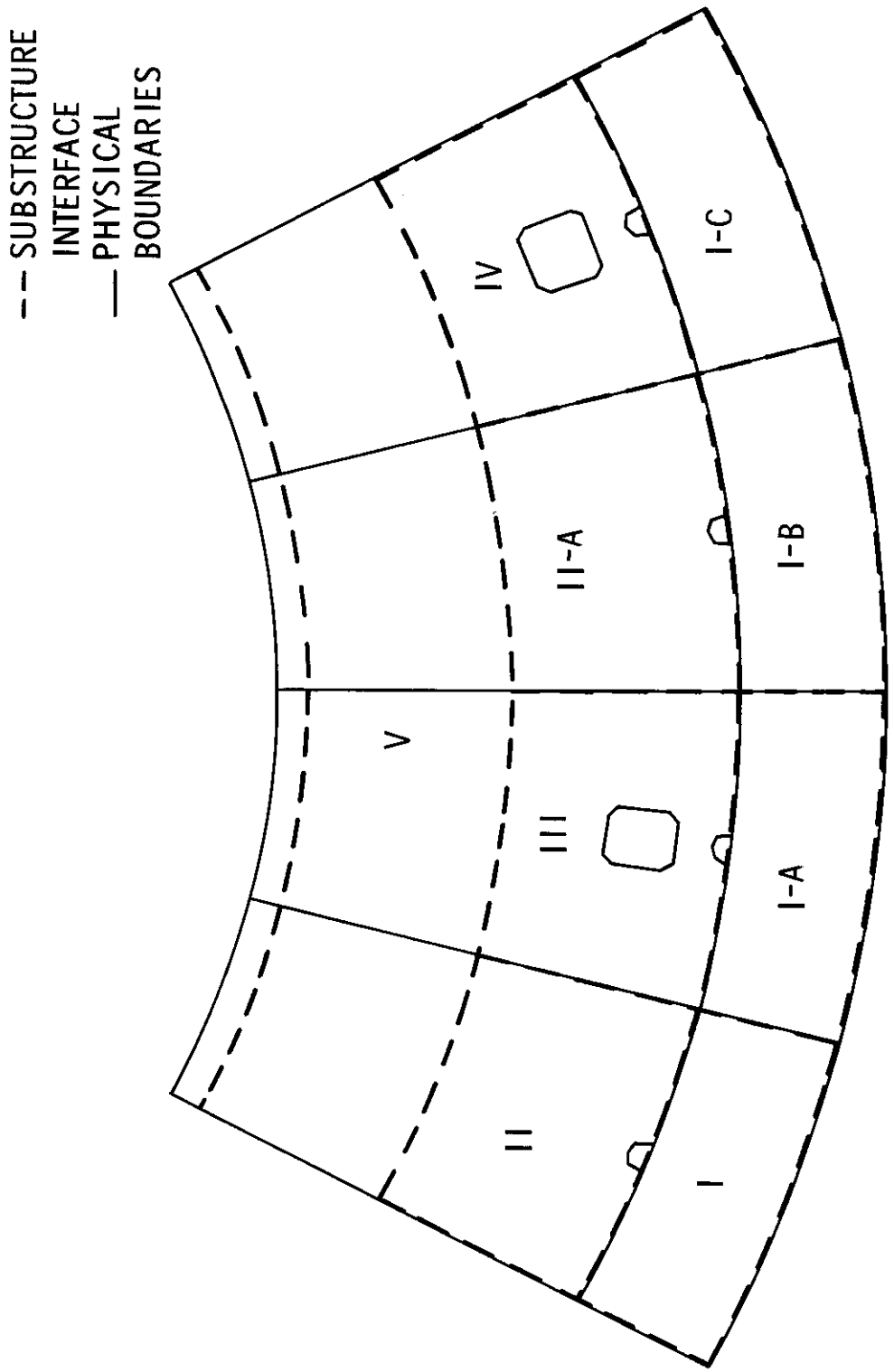

Figure 10. SLA Substructure Breakdown

Idealization sufficiently refined to permit meaningful interpolation of stress distributions, implies consideration of all significant variations in overall configuration, sizing dimensions, material properties, thermal loading, intertial loading, special connections and boundary conditions. These factors provide the most direct guidance to the idealization.

The end of first stage boost (End-Boost) loading is comprised of thermal and inertial loading. The thermal loading is confined to the outer sandwich shells of the SM/SLA Structure. A complex, nonaxisymmetric temperature distribution exists over this surface by virtue of the structural variations. For example, the reaction control panels cause local disruptions to to the temperature as do the numerous backup stiffeners and the externally bonded insulation. Variations in the thermal gradient through the sandwich shells accompany the surface variations in temperature.

The inertial loading is comprised of a high axial-g component and a relatively small lateral-g component. This loading gives rise to axial, shear and bending moments at the interface of the SM Structure with the CM Structure. Inertial loads arising within the SM/SLA Structure are realistically distributed to adjacent gridpoints.

This summary of applied loading is completed by stating that the SM/SLA Structure was elastically supported and bounded at the bottom of the SLA Structure. The complex variabilities of the SM and SLA Structures are apparent in Figures 2 and 3 thus narrative description is omitted.

The resultant substructure idealizations are shown as a group in Figure 11 for the SLA Structure. Dashed lines again denote substructure breakdown. The construction of the SM Structure does not permit a picture such as this. Instead, an indication of the SM Structure idealization is given via computer drawn plots of representative outer shell, radial beam and aft bulkhead substructures in Figures 12, 13, and 14. The outer sandwich shell is built-up of shell elements and the radial beam contains axial force members, frames and shear panels. The aft bulkhead is comprised of a triangular prism core with membrane face sheets. A detailed description of all substructures is given in Reference 1. These substructures are assembled into the skeleton of substructure interface lines shown in Figure 15 to form the finite element model of the SM/SLA Structure.

The assembled structural model of the SM/SLA Structure exceeded the capacity of the automated system in terms of the number of interface degrees of freedom. For this reason,

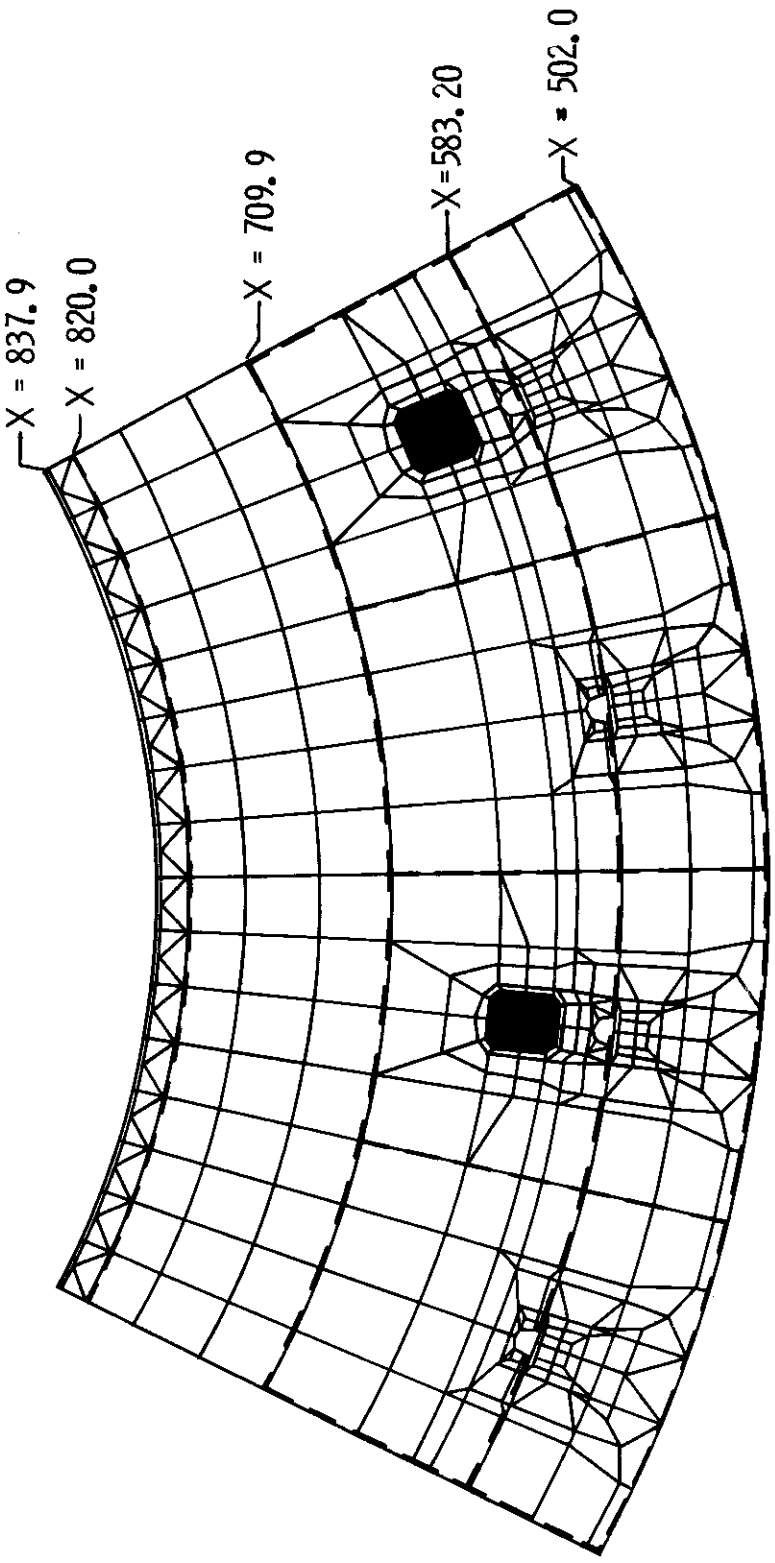

Figure 11. SLA Stabilization

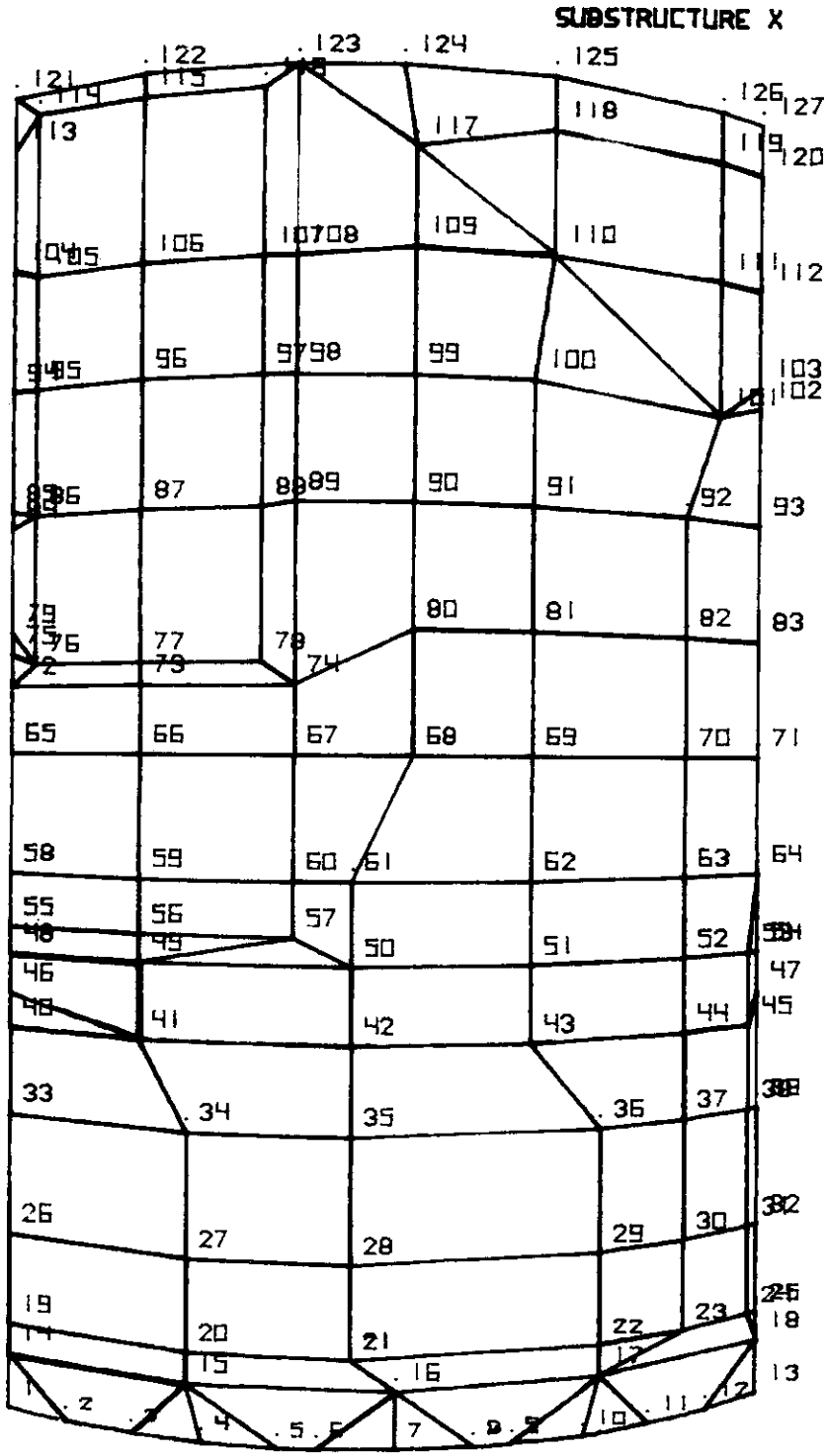

Figure 12. SM Outer Shell Subplot

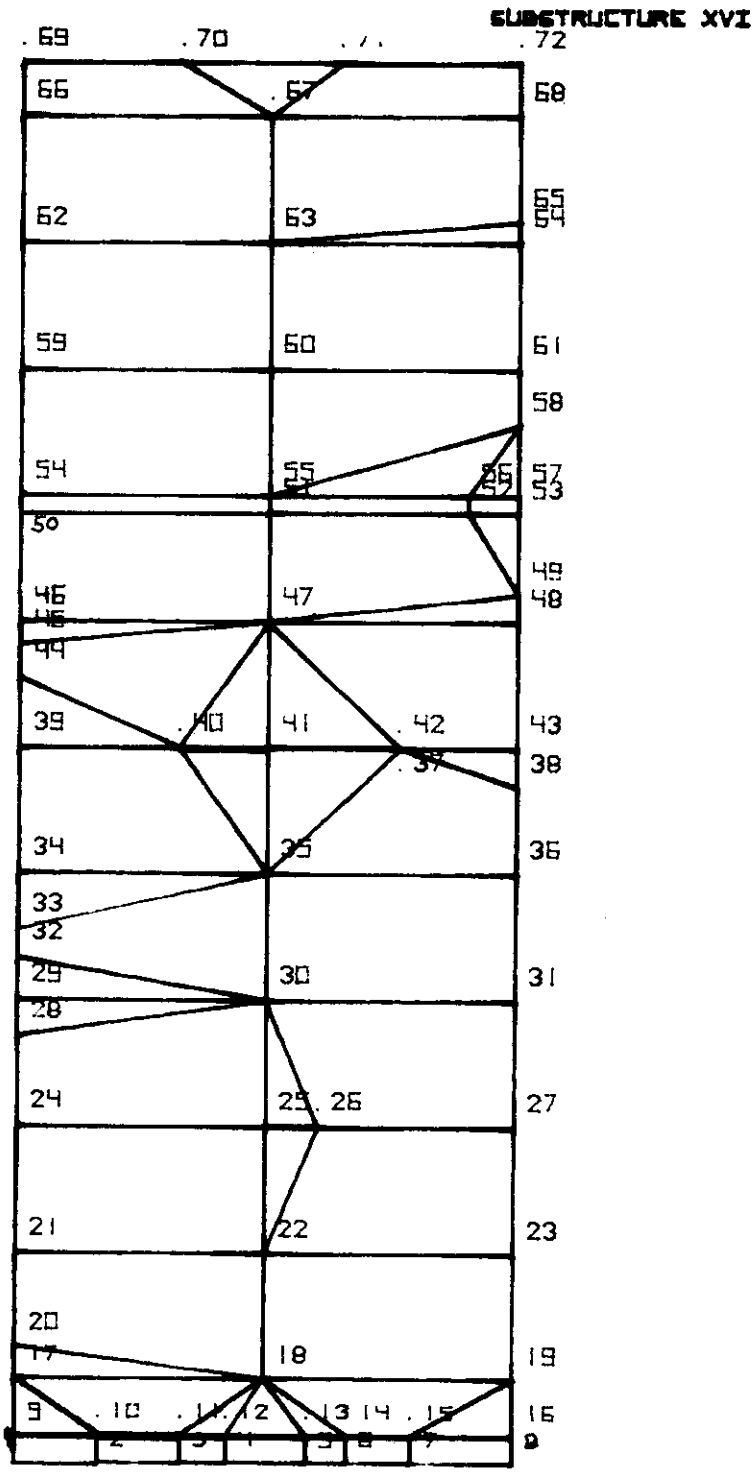

Figure 13. SM Radial Beam Subplot

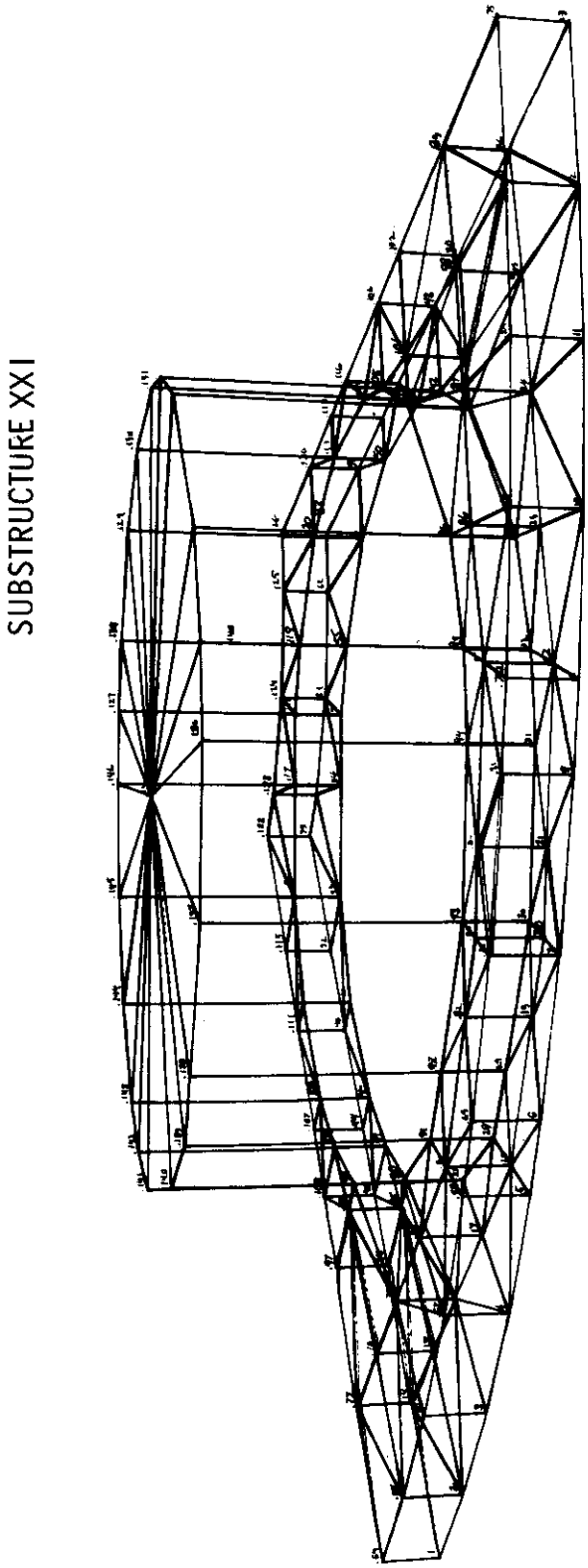

Figure 14. SM Aft Bulkhead Subplot

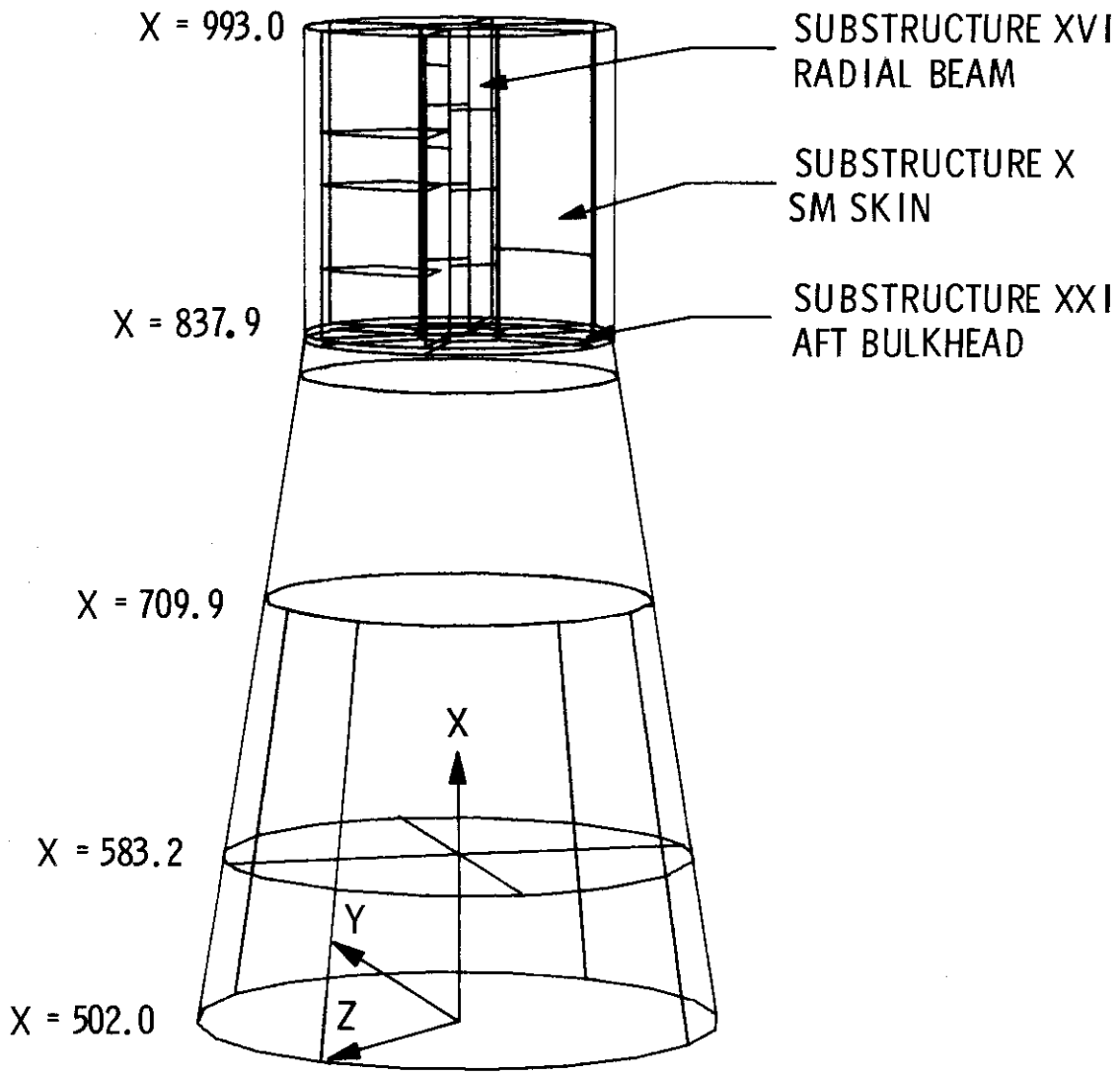

Figure 15. Substructure Interfaces

it was necessary to execute the analysis in two parts. In the first part, the SM Structure was simulated and SM loads were applied at the top of the SLA Structure. Analysis of this SLA portion was conducted. Then, the portion of SM/LA Structure aft of Station x = 709.9 was deleted and the forward portion was analyzed. An overlap of 110 inches was common to these two analyses which proved, as is shown in Section V, to be sufficient to obtain accurate results over the entire structure.

SECTION VI

SUMMARY OF RESULTS

The first results obtained in proceeding through the four-phase analysis process are predictions of the behavior induced within individual substructures with the interface grid-points held fixed. These results often approximate the final solution; however, this was not the case for the SM/SLA Structure. In this case, the Phase I results were useful only to the extent of confirming the subsets of equations as solveable. Small force-balance residuals were obtained for all of the SM/SLA Phase I analyses. This tends to confirm the suitability of the finite element model of the total structure.

Phase II of the analysis process is the primary equation solving step. This is the crucial test of the finite element model and numerical solution technique. Beyond this point the analysis process is one of backsubstitution for secondary variables. One good test of the accuracy of this analysis phase is to check gross force-balance of the applied loads and reactions. Since the Phase II analysis was conducted in two parts, corresponding to overlapping fore and aft sections of the SM/SLA Structure, two Phase II gross force-balance checks can be made.

Figure 16 exhibits a free-body diagram of the aft section showing the gross force-balance achieved in the aft section Phase II analysis. Focusing upon the axial force resultant that is the most readily manually generated, a percentage difference of 0.2% is disclosed. This level of accuracy is excellent for the size of problem considered.

Figure 17 exhibits the corresponding force-balance diagram for the overlapping fore section. The same level of accuracy is demonstrated for this larger portion of the Phase II solution. A total of 1691 degrees of freedom was included in this Fore Section Phase II analysis.

In an engineering environment the measure of a successful analysis is the validity of the predicted stress behavior. "Valid" is necessarily interpreted as "rational" in the absence of reliable alternative predictions of stress behavior.

Only a limited presentation of the thermal stress results for the SM/SLA Structure can be offered in the present context. In an attempt to make this summary presentation as conclusive as possible, the region of overlap between the Phase II SLA and SM/SLA models is examined herein.

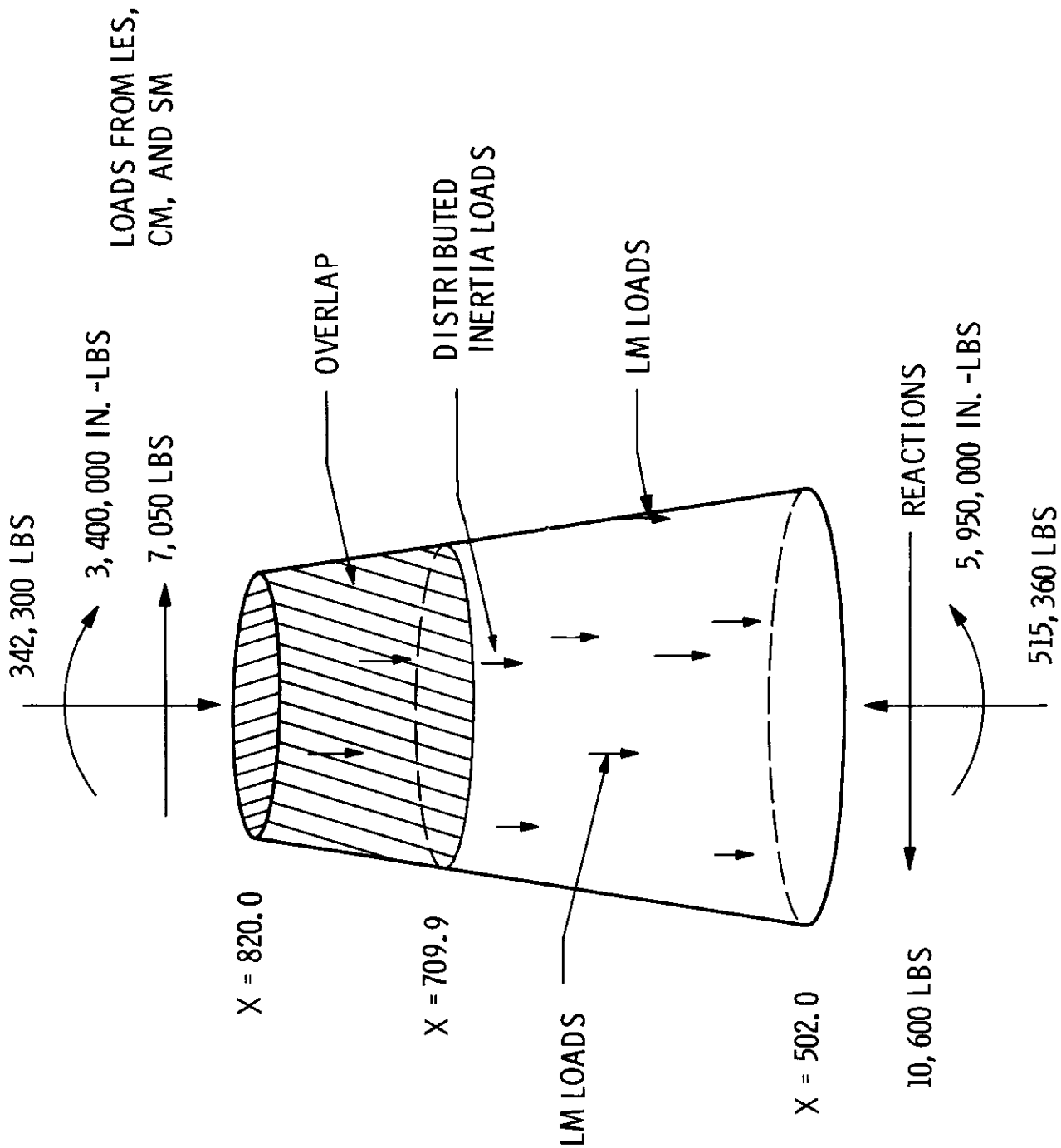

Figure 16. Aft Section Force Balance

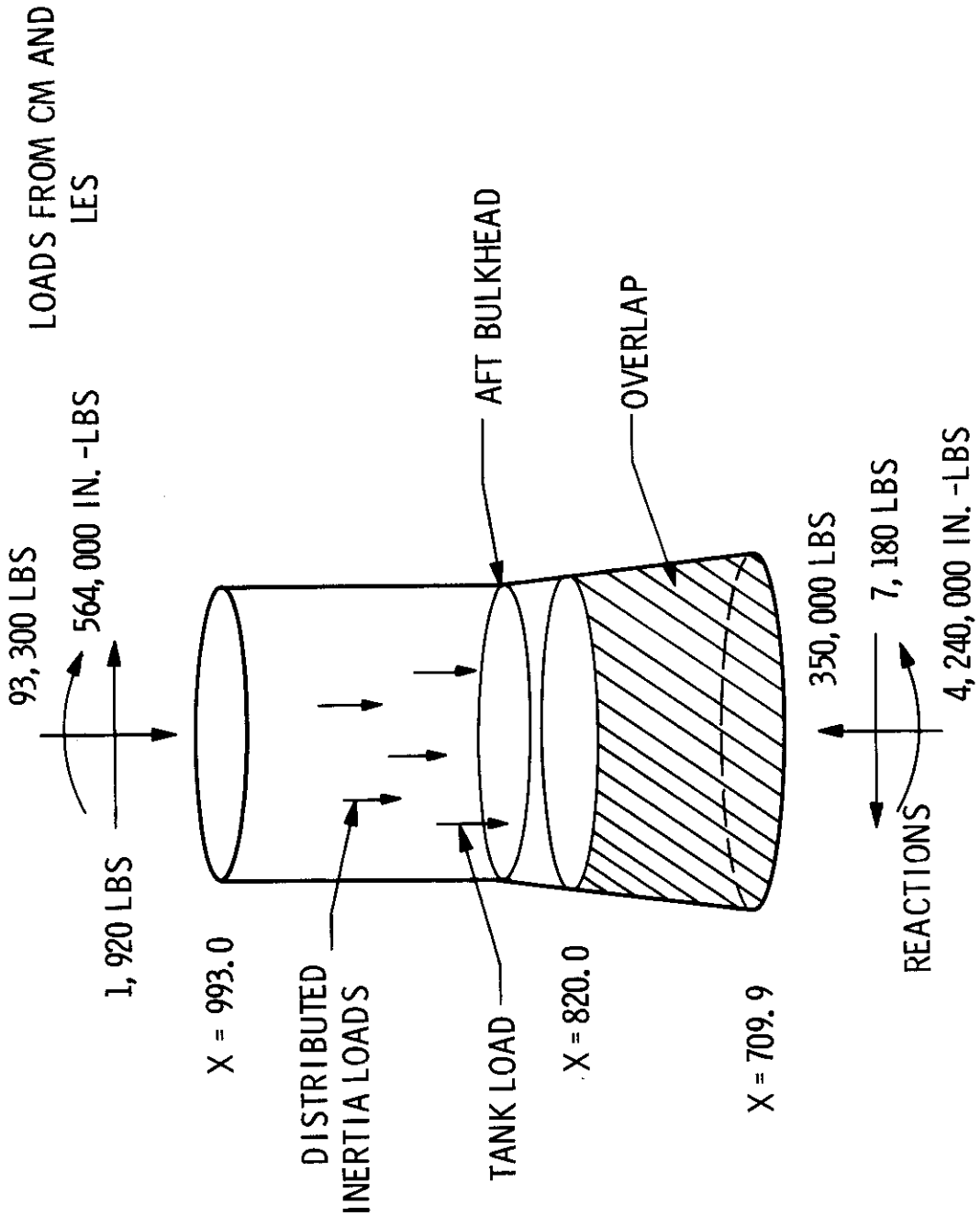

Figure 17. Fore Section Force Balance

Figure 18 presents a comparison of stress behavior predictions from the fore and aft section analyses at the middle of the overlap. Specifically, the alternative circumferential profiles of the axial stress resultant N_x are presented. If the close agreement sought at this axial position is realized, then, results forward of this axial station can be accepted with confidence from the fore section analysis and results aft of this axial station can be accepted with confidence from the aft section analysis.

Observation of Figure 18, shows the two profiles of axial stress resultant to be in general agreement. Both exhibit the expected correlation with a beam theory approximation. This underscores the good gross force-balance.

Both finite element based profiles in Figure 18 exhibit secondary waves about the basic cosine wave of the beam theory approximation. The capability to predict these local variations is the justification of the finite element analyses. The differences between the two finite element based profiles are readily explained by comparison of the fore and aft section models.

The profile of N_x derived from the aft section analysis is extracted from Figure 18 and reproduced in Figure 19 with the important structural characteristics of the aft section noted. Major structural reinforcements noted include the longitudinal interpanel splices, the LM attachment area and the major access doors.

The axial stress resultant is observed to increase above the hard points in the shell at the LM attachment and access door areas. Conversely, a decrease is observed at the longitudinal splices where the backup discrete stiffeners serve to relieve the shell load. Thus, the aft section stress profile correlates rationally with the model.

The profile of N_x, derived from the fore section analysis, is extracted from Figure 18 and reproduced in Figure 20 with the positions of the SM radial beams noted. Local effects of the radial beams are observed to have been attenuated at the axial station considered. The generally lower load in the region between radial beams 4 and 6 in comparison with the region between radial beams 1 and 3 is attributed to the lighter oxidizer sump and fuel tanks in the former region.

The foregoing examination of Figures 19 and 20 has shown that the discrepancies between the two results from sophistication in the finite element models rather than from inaccuracy of the solution. The comparison at the middle of the overlap is considered satisfactory and the results removed from this region are accepted without reservation.

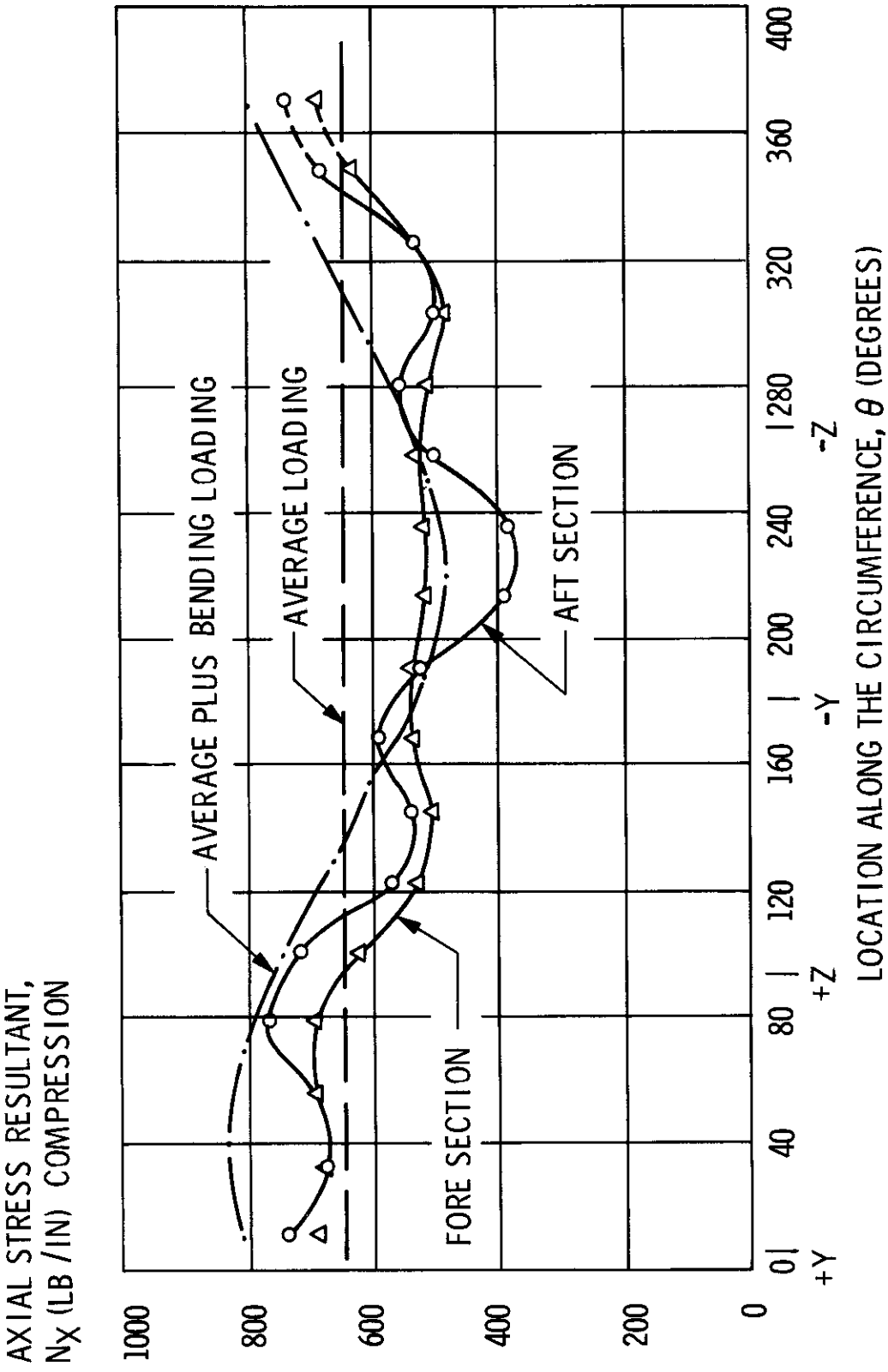

Figure 18. Axial Stress Resultant, N_X Versus Circumferential Location, for Inertial Loading at X = 765.0

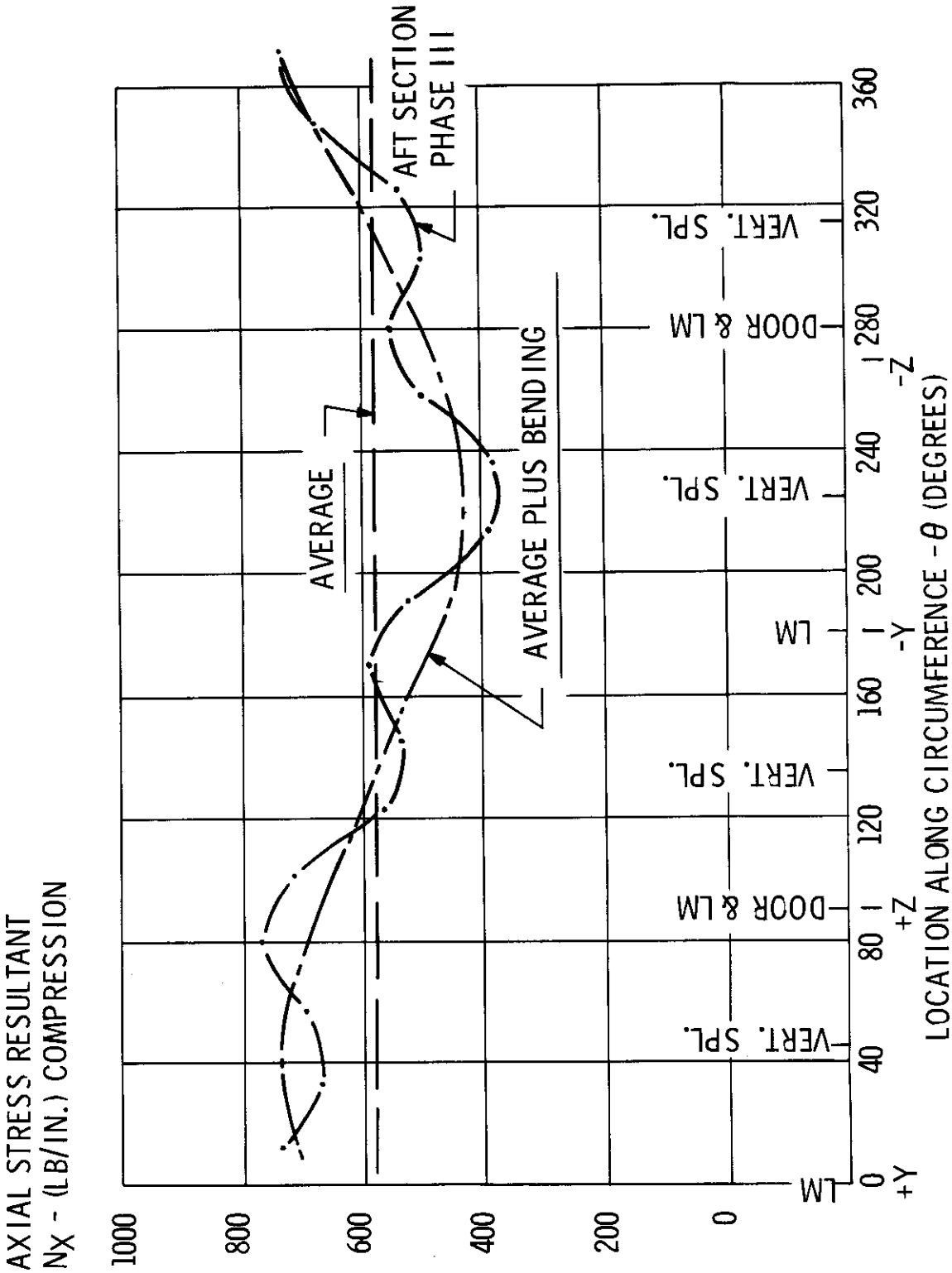

Figure 19. Axial Stress Resultant, N_X Versus Circumferential Location, Inertial Loading at X = 765.0 in the Aft Section

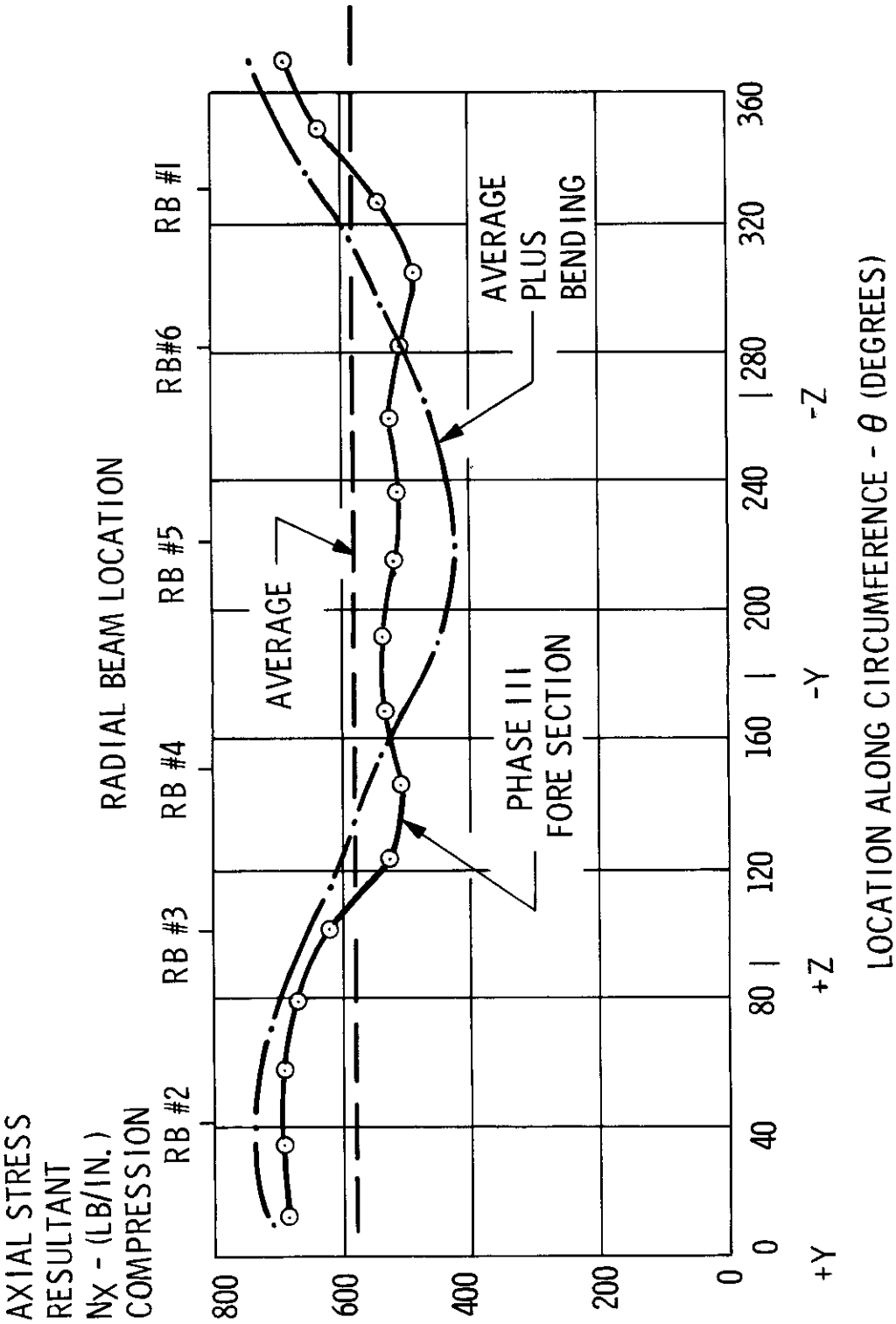

Figure 20. Axial Stress Resultant, N_X Versus Circumferential Location, for Inertial Loading at Sta 765.0 in the Fore Section

The foregoing paragraphs examined the axial stress resultant via a profile taken around the circumference at a given station. Figure 21 presents a similar profile taken along the meridian of the SM/SLA Structure at a given circumferential position. An angular position of $\theta = 55°$ ($+Y_{sc} = 0°$) was chosen for convenience in extracting the required stress resultant data. This angle places the profile close to radial beam 2 in the SM Structure and approximately midway between two LM attachement points in the SLA Structure. Structural items that affect the local stress distribution are noted on the profile of Figure 21.

With reference to Figure 21, the axial stress resultant in the shell is observed to begin near zero at the interface with the CM Structure. This is consistent with the design of the interface. Moving aft, the load builds up initially then decreases at the radiator panel where the outer face sheet thickness is increased sixfold.

A sharp rise in the axial shell stress resultant is noted at the interface between the SM and SLA Structures as the SM tank loads are transferred through the aft bulkhead out to the SLA shell.

Moving aft through the SLA Structure, an increase in gross bending tends to increase the axial stress resultant. A hand calculation readily confirms that this is offset by the increasing diameter to yield the profile of Figure 21 for this region. Note that the alternative predictions through the overlap region are in good agreement.

A marked increase in the stress resultant arises in moving aft through the LM attachment station. This increase might be expected to be even higher except that the angular position is well removed from the LM attachment points and the face sheet thicknesses in the aft SLA are increased.

The foregoing results, taken together with other results not presented, have proved rational upon examination without exception and are taken to confirm the validity of the analysis. Validity is presumed in presenting limited additional results.

The objective established at the outset was to obtain detailed stress predictions and meaningful margins of safety from the subject primary analysis. To demonstrate the success in this regard, attention is focused upon the region of a major access hatch in the SLA Structure identified as Substructure III and recorded in Figure 22.

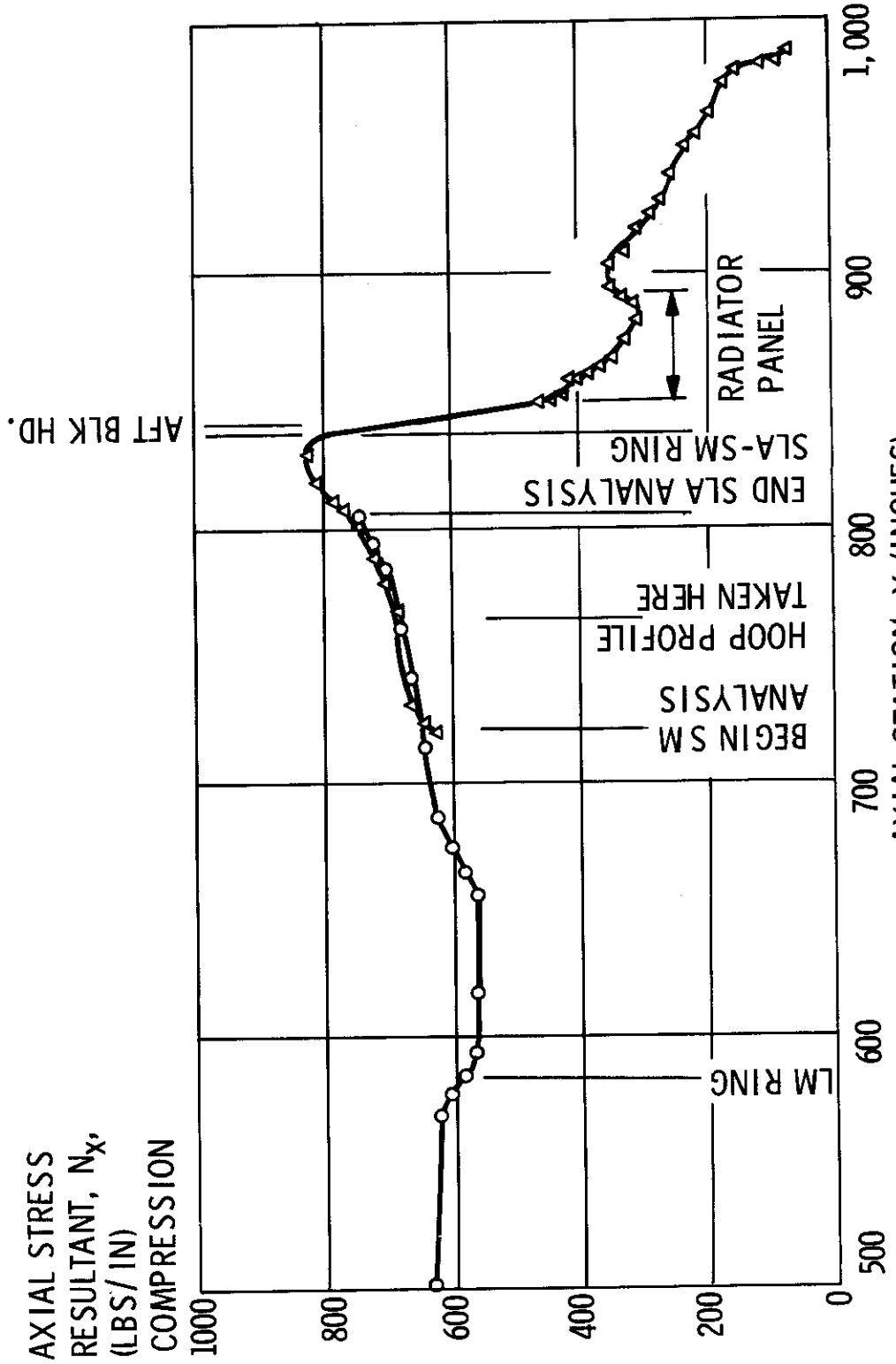

Figure 21. Axial Stress Resultant Profile at θ = 55 Degrees

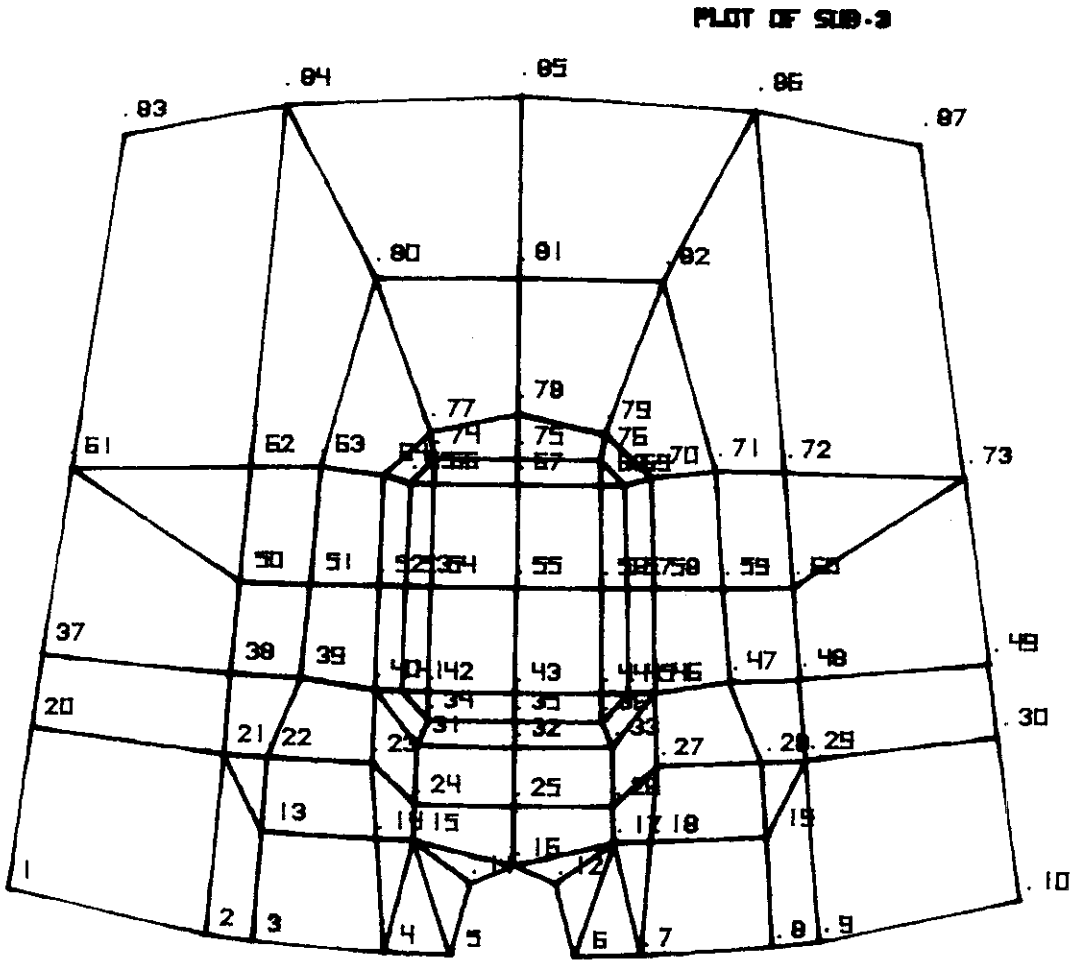

Figure 22. SLA Substructure III Idealization

The access hatch in Substructure III is assumed structural. The shell construction is sandwich. Stresses are predicted at the center and corners of both the inner and outer face sheets. Contours of axial stress predicted in the outer-face sheet are shown in Figure 23.

The high degree of refinement inherent in the predicted axial stress distribution is clear in Figure 23. Usefulness of such a display for quantitative interpretation is limited. However, it is evident that the surrounding reinforcement tends to bridge the load around the door of the access hatch.

The voluminous data underlying predicted stress distributions such as illustrated in Figure 23 defies manual reduction to margins of safety. This problem was circumvented in this analysis. All data reduction was performed by automated data reduction routines and automated search routines to flag negative margins of safety.

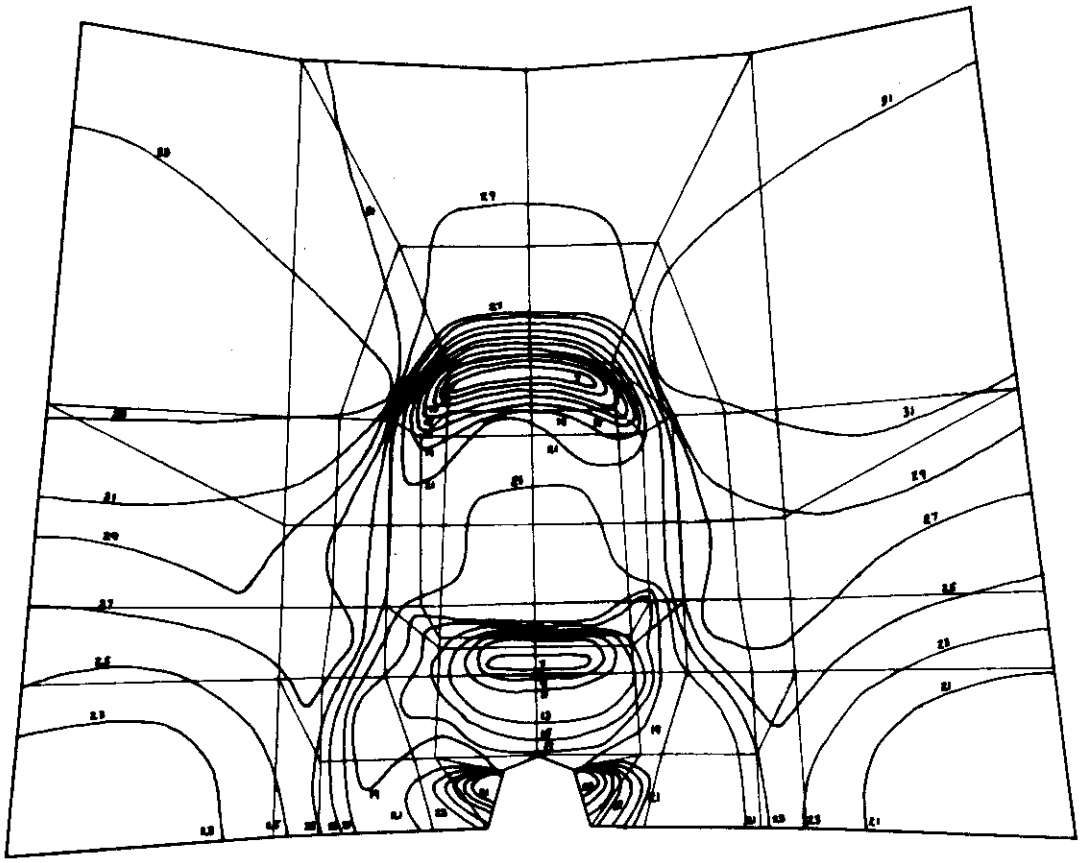

Figure 23. Substructure III Outerface Sheet Axial Stress Distribution - KSI

A typical output display of reduced data is included as Figure 24. This output display is referred to as "stress report" output. Such sheets form the primary information package from the finite element stress analysis to the stress analyst. Having this stress report output, the stress analyst can focus his attention on the analysis of joints and attachments. Accordingly, the body of the stress report (Reference 2) prepared in the subject thermal stress analysis of the Apollo SM/SLA Structure, is devoted primarily to analysis of joints and attachments using the force distributions predicted with the finite element model. The basic structure is evaluated in depth directly by the foregoing stress report output from the finite element analysis.

The facility of the Bell automated analysis system and associated structural analysis practices for dealing with large scale structures has been well demonstrated by the stress analysis of the Apollo SM/SLA Structure. Simpler structures generally do not permit use of this approach; however, an application is appended here to illustrate that substructuring may be useful on small structures.

ELEMENT NO. 109 PLLG NO. 2 LOAD CONDITION NO. 5
MATERIAL 221206234165 AVERAGE ELEMENT TEMPERATURE 0.29367E 03

STRESS RESULTANTS AT CENTROID

MEMBRANE STRESSES			FLEXURAL STRESSES		
N_x	N_y	N_{xy}	M_x	M_y	M_{xy}
0.43666E 02	-0.55454E 03	-0.60961E 02	0.49376E 01	-0.13592E 03	-0.29973E 02

SANDWICH ANALYSIS ---- THICKNESS 0.10000E 01

UPPER PLATE ANALYSIS				LOWER PLATE ANALYSIS		
0.37700E 03			PLATE TEMPERATURE	0.21033E 03		
0.16000E-01			PLATE THICKNESS	0.10000E-01		
σ_x	σ_y	τ_{xy}		σ_x	σ_y	τ_{xy}
0.19881E 04	-0.33732E 05	-0.42117E 04	STRESSES	0.13709E 04	-0.16617E 05	-0.47763E 03
σ_{p1}	σ_{p2}	$\left(\frac{\sigma_x+\sigma_y}{2}\right)$	PRINCIPLE	σ_{p1}	σ_{p2}	$\left(\frac{\sigma_x+\sigma_y}{2}\right)$
0.24779E 04	-0.34222E 05	-0.15872E 05	STRESSES	0.13835E 04	-0.16630E 05	-0.76232E 04
-0.66344E 01			STRESS ANGLE(DEG.)	-0.15199E 01		
0.35526E 05			EQLIVALENT STRESS	0.17363E 05		
0.18350E 05			MAXIMUM SHEAR STRESS	0.90067E 04		

MARGINS OF SAFETY *

VON MISES

1	0.27625E 00	1	0.21571E 01
2		2	

MAXIMUM SHEAR STRESSES

3	0.46196E 00	3	0.25767E 01
4		4	

MAX. PRIN. STRESSES

5	0.32487E 00	5	0.22963E 01
6		6	

STRESS RATIO METHOD

7	0.58210E 01	7	0.33982E 02

*ULTIMATE LOAD AND MARGIN OF SAFETY

Figure 24. Phase IV Stress Report Output

Figure 25 shows the neck region of a double-walled tank assembly. The two walls are joined in the neck through three circumferential welds. A photomicrograph of a representative weld cross section is shown in Figure 26. Of interest was the load transfer mechanism of the tri-weld connection and the detailed stress distributions induced in the regions of the welds.

The potentially large number of finite elements and degrees of freedom necessary to perform this analysis were avoided using the analysis practices described herein. The structure was divided into two typical subsections. These distinct subsections were idealized as substructures as shown in Figure 27.

Two Phase I analyses were performed. The two interface referenced substructure models were then each assembled four times as shown in Figure 28 and the Phase II analysis was performed. The Phase III backsubstitutions for the stresses completed the analysis. This approach minimized the preparation of input data and permitted execution in a fraction of the time that would have been required using a more conventional approach. Thus, relatively small problems can also benefit from the structural analysis practices put forward herein.

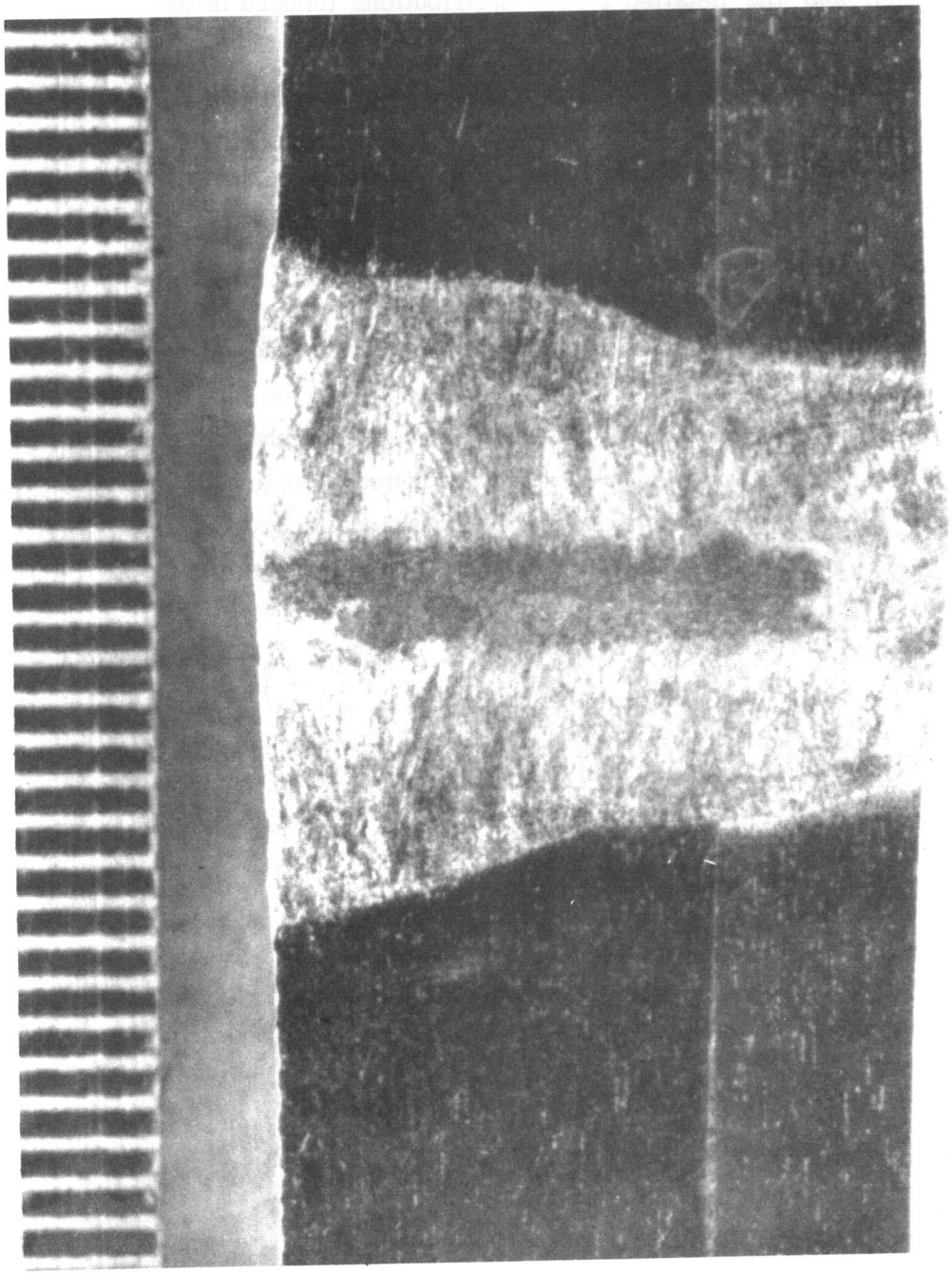

Figure 25. Photomicrograph of Weld Cross Section, 15X Magnification

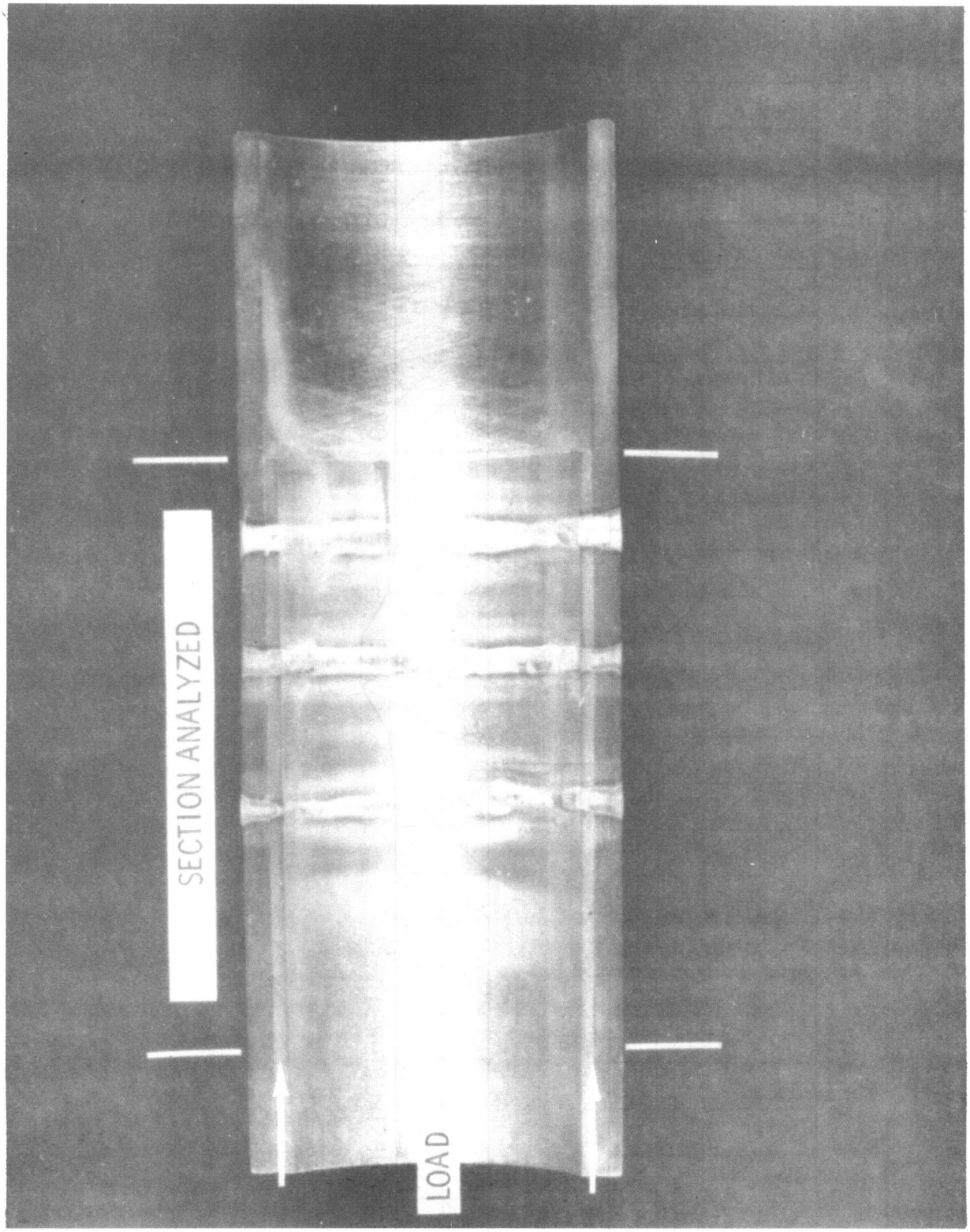

Figure 26. Neck Region of Double Walled Tank Assembly

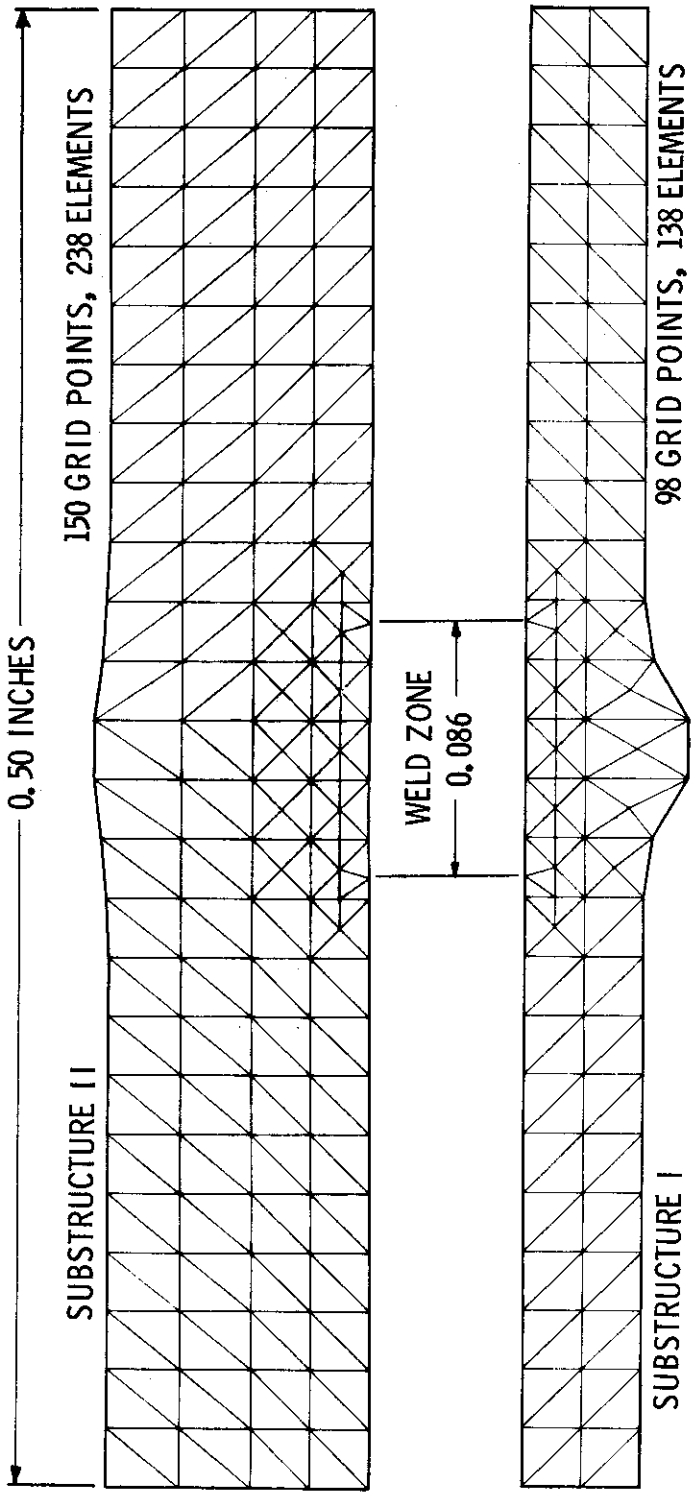

Figure 27. Typical Weld Joint Substructures

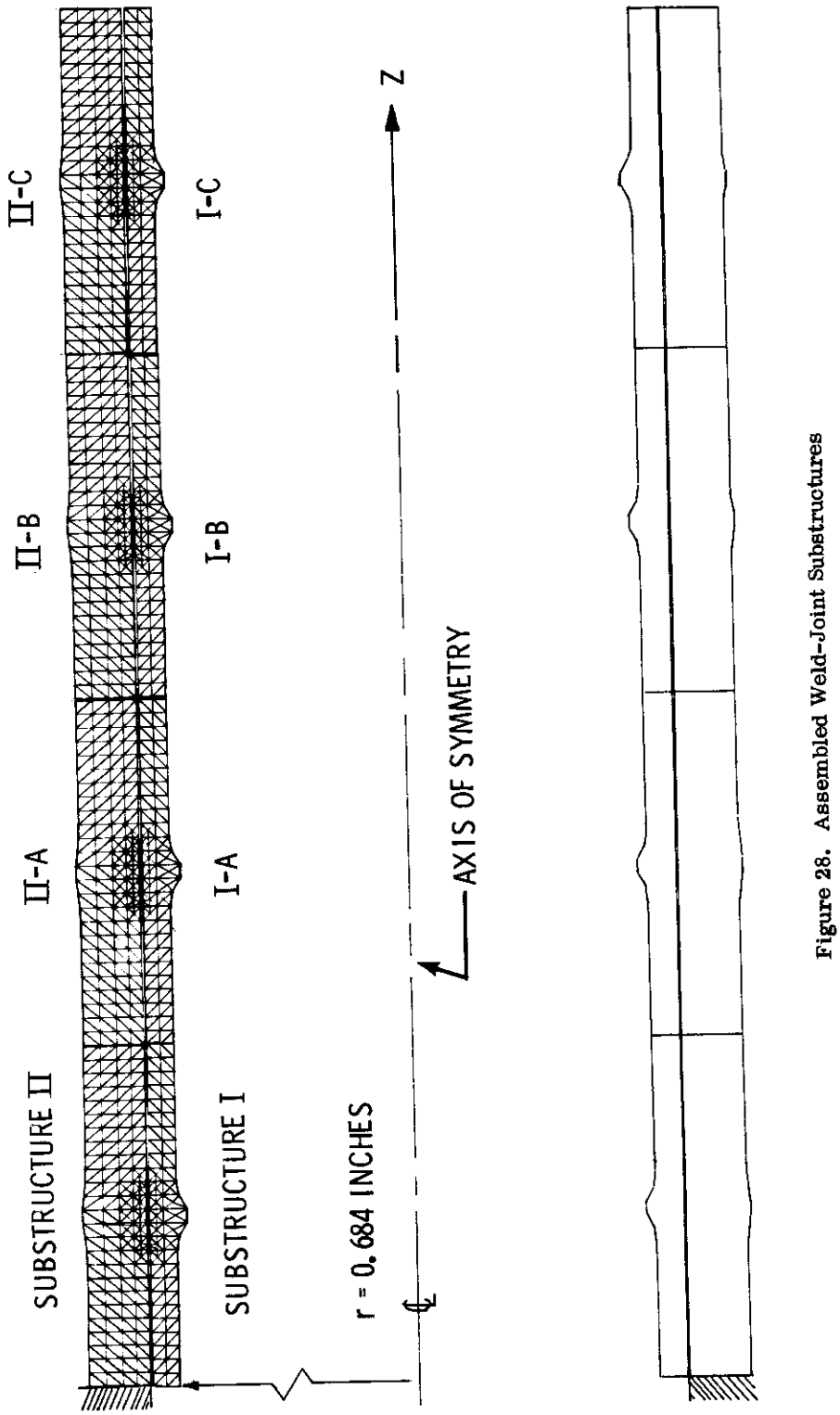

Figure 28. Assembled Weld-Joint Substructures

SECTION VII

CONCLUSIONS

The matrix methods of structural analysis based upon finite element idealization offer the opportunity to provide improved analysis support to the structural design process. A powerful implementation of these methods was described herein. Substructuring was put forward as a practical approach to efficient utilization of the finite element methods in the context of large scale structures. The asserted capability of the automated analysis system and effectiveness of the analysis practices based upon substructuring are concluded to be validated by the analysis of the stacked Apollo SM/SLA Structure.

SECTION VIII

REFERENCES

1. Mallett, R. H., and Braun, F. W., Thermal Stress Analysis of the Apollo Block II Spacecraft Lunar Module Adapter and Service Module. Volume I: Finite Element Analysis, Bell Aerosystems Contract Report No. 2373-941001, June 1968.

2. Meholick, W., Thermal Stress Analysis of the Apollo Block II Spacecraft Lunar Module Adapter and Service Module. Volume II: Stress Report, Bell Aerosystems Contract Report No. 2373-941002, Jume 1968.

3. Jones, R. M., Editor, Proceedings of the Nosetip Stress Analysis Technical Interchange Meeting, Space and Missile Systems Organization Air Force Systems Command, Report No. SAMSO-TR-67-108, November 1967.